

Decomposition in Decision and Objective Space for Multi-Modal Multi-Objective Optimization

Monalisa Pal and Sanghamitra Bandyopadhyay*

Abstract

Multi-modal multi-objective optimization problems (MMMOPs) have multiple subsets within the Pareto-optimal Set, each independently mapping to the same Pareto-Front. Prevalent multi-objective evolutionary algorithms are not purely designed to search for multiple solution subsets, whereas, algorithms designed for MMMOPs demonstrate degraded performance in the objective space. This motivates the design of better algorithms for addressing MMMOPs. The present work identifies the crowding illusion problem originating from using crowding distance globally over the entire decision space. Subsequently, an evolutionary framework, called graph Laplacian based Optimization using Reference vector assisted Decomposition (LORD), is proposed, which uses decomposition in both objective and decision space for dealing with MMMOPs. Its filtering step is further extended to present LORD-II algorithm, which demonstrates its dynamics on multi-modal many-objective problems. The efficacies of the frameworks are established by comparing their performance on test instances from the CEC 2019 multi-modal multi-objective test suite and polygon problems with the state-of-the-art algorithms for MMMOPs and other multi- and many-objective evolutionary algorithms. The manuscript is concluded by mentioning the limitations of the proposed frameworks and future directions to design still better algorithms for MMMOPs. The source code is available at <https://worksupplements.droppages.com/lord>.

Keywords: Multi-Modal Multi-Objective Optimization; Non-dominated Sorting; Crowding Distance; Reference vector based Decomposition; Graph Laplacian

*M. Pal and S. Bandyopadhyay are with Machine Intelligence Unit, Indian Statistical Institute, 203 Barrackpore Trunk Road, Kolkata - 700108, West Bengal, India. E-mail: M. Pal (monalisap90@gmail.com) and S. Bandyopadhyay (sanghami@isical.ac.in). This work has been partially supported by Indian Statistical Institute, Kolkata. It has also been supported by J. C. Bose Fellowship (SB/SJ/JCB-033/2016) from Department of Science and Technology, Government of India. This version corresponds to the accepted manuscript (DOI: 10.1016/j.swevo.2021.100842) at <https://www.sciencedirect.com/science/article/abs/pii/S2210650221000031>.

1 Introduction

Multi-objective optimization deals with problems having two or more conflicting objectives (optimization criteria) [1, 2]. The mathematical formulation of a box-constrained multi-objective minimization problem (1) presents the mapping from a N -dimensional vector ($\mathbf{X} = [x_1, \dots, x_N]$) in the decision space (\mathcal{D}) to a M -dimensional vector ($\mathbf{F}(\mathbf{X})$) in the objective space [1, 2].

$$\begin{aligned} &\text{Minimize } \mathbf{F}(\mathbf{X}) = [f_1(\mathbf{X}), f_2(\mathbf{X}), \dots, f_M(\mathbf{X})] \\ &\text{where, } \mathbf{X} \in \mathcal{D} (\subseteq \mathbb{R}^N), \mathbf{F}(\mathbf{X}) : \mathcal{D} \mapsto \mathbb{R}^M \\ &\text{and } \mathcal{D} : x_j^L \leq x_j \leq x_j^U, \forall j = 1, 2, \dots, N \end{aligned} \quad (1)$$

Pareto-dominance relation is used for comparison of two vectors, i.e., \mathbf{X} Pareto-dominates \mathbf{Y} , as defined below.

$$\begin{aligned} &\forall i \in \{1, 2, \dots, M\}, \text{ and } \exists j \in \{1, 2, \dots, M\}, \\ &\mathbf{X} \prec \mathbf{Y} \iff (f_i(\mathbf{X}) \leq f_i(\mathbf{Y}) \wedge f_j(\mathbf{X}) < f_j(\mathbf{Y})) \end{aligned} \quad (2)$$

A Pareto-optimal solution $\mathbf{X}^* \in \mathcal{D}$ is attained, if $\nexists \mathbf{X} \in \mathcal{D}$ that dominates \mathbf{X}^* . A set of all such Pareto-optimal solutions form the Pareto-optimal Set (PS) and their images in the objective space yield the Pareto-Front (PF) [1, 2].

The notion of Multi-Modal Multi-Objective Problem (MMMOP) [3] arises when a set of k_{PS} (≥ 2) distinct decision vectors ($\mathcal{A}_M = \{\mathbf{X}_1, \mathbf{X}_2, \dots, \mathbf{X}_{k_{PS}}\}$) maps to *almost same* objective vectors, i.e., $\forall (\mathbf{X}_i, \mathbf{X}_j) \in \mathcal{A}_M \times \mathcal{A}_M, \|\mathbf{F}(\mathbf{X}_i) - \mathbf{F}(\mathbf{X}_j)\| < \epsilon$ (a small number) as illustrated in Fig. 1 for a benchmark test problem (MMF4 [4]). Thus, the PS can consist of multiple subsets of non-dominated solutions, where each subset can independently generate the entire PF.

Research on MMMOPs is motivated to discover those k_{PS} alternative solutions for nearly the same objective values to facilitate the comparison of non-numeric, domain-specific attributes of these equivalent solutions during decision-making. Moreover, when the practical implementation of a solution is hindered, a nearly equivalent alternative can be beneficial. Such MMMOPs are seen in rocket engine design [5], feature selection [6] and path-planning problems [7].

To optimize such MMMOPs, an Evolutionary Algorithm (EA) faces the following challenges:

1. Maintaining diversity in the decision space, i.e., representing and maintaining diversity within each of the multiple solution subsets which independently maps to a diverse approximation of the PF.
2. Necessity of a large population to efficiently represent an MMMOP. For example, if k_{PF} points (e.g., 100) represent a 2-objective PF and k_{PS} decision vectors

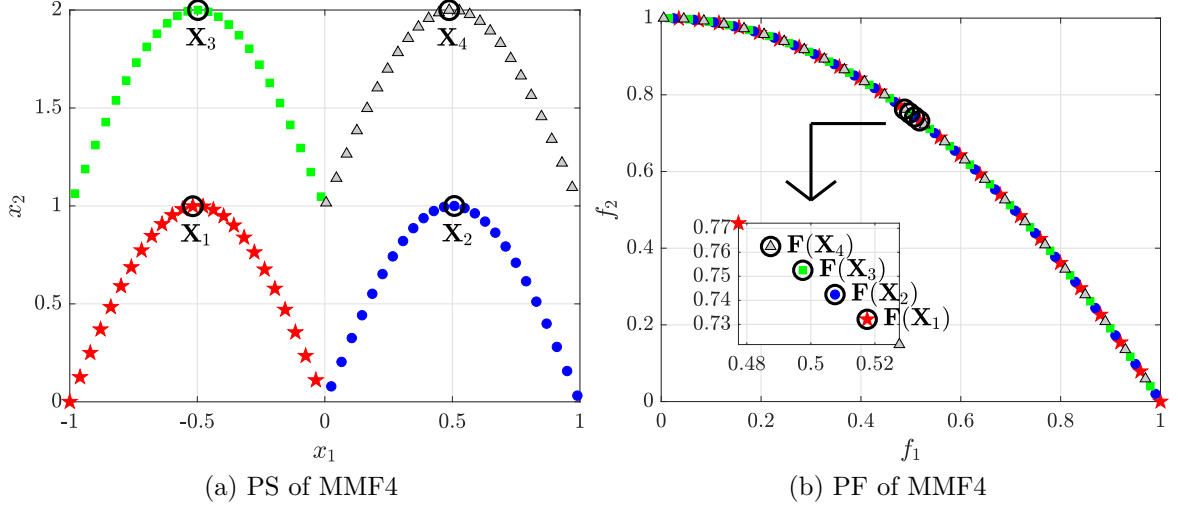


Figure 1: Four solution vectors ($\mathbf{X}_1, \mathbf{X}_2, \mathbf{X}_3$ and \mathbf{X}_4) mapping to *almost same* objective vectors ($\mathbf{F}(\mathbf{X}_1), \mathbf{F}(\mathbf{X}_2), \mathbf{F}(\mathbf{X}_3)$ and $\mathbf{F}(\mathbf{X}_4)$) for a benchmark test problem (MMF4 [4]).

(e.g., 4 for MMF4 problem [4, 8]) map to each point of the PF, then the final population size required is $k_{PF} \times k_{PS}$ (e.g., $100 \times 4 = 400$).

Such MMMOPs cannot be tackled by any of the existing Multi-Objective Evolutionary Algorithms (MOEAs) [2, 1]: Pareto-dominance based EAs (such as NSGA-II [9] and θ -DEA [10]), indicator-based EAs (such as HypE [11] and GDE-MOEA [12]) and decomposition-based EAs (such as MOEA/D [13], NSGA-III [14] and MOEA/DD [15]), as these MOEAs focus primarily on the objective space to regulate the population, overlooking the solution distribution in the decision space.

For decomposition-based EAs, Das and Dennis’s approach [16] is used which involves a two-layered recursive procedure to define reference vectors from the origin to a set of uniformly distributed points on a unit hyperplane in the objective space. These reference vectors partition the objective space into multiple sub-spaces and thereby, reduces the problem complexity by restricting one or more steps of the EA within these subspaces [17]. As these algorithms neither suffer from the reduced selection pressure in high dimensional objective space like Pareto-dominance based EAs [1, 2] nor require the extreme computational effort for hypervolume-like indicator evaluation [11], decomposition based EAs are extensively used for M -objective problems.

Omni-optimizer [18] is the earliest work to consider the solution diversity in the

decision space¹. It uses of crowding distance in the decision space (CDX) after the non-dominated sorting [18] but hampers the solution diversity in the objective space. The work in [19] uses neighborhood count and Lebesgue contribution to promote solution diversity in the decision and objective spaces, respectively. However, its evaluation involves large computational cost. The work in [20] considers CDX and a probabilistic model to estimate PS and PF but performs poorly when PS is a linear manifold.

Extensive research on EAs for MMMOPs (MMMOEAs) started with decision-niched NSGA-II (DN-NSGA-II) [21] which replaces the crowding distance in the objective space (CDF) with CDX in NSGA-II. Thus, the diversity of solutions in the objective space receives a significant setback. Another study combines NSGA-II with Weighted Sum Crowding Distance and Neighborhood Based Mutation (NSGA-II-WSCD-NBM) [22] for addressing MMMOPs. Unlike these preliminary MMOEAs, MO_Ring_PSO_SCD [23] establishes that diversity preservation and niching methods (like ring topology) play vital roles for MMMOPs. Although computationally expensive (exponential with the number of decision variables), Zoning search (ZS) [24] enhance diversity in the decision space. MOEA/D with addition and deletion operators (MOEA/D-AD) [25] introduces the notion of *almost same* Pareto-optimal solutions. Its recent extension (ADA) [26] proposes adaptive tuning of K (number of equivalent solutions per subspace) for its operation. Multi-Modal Multi-objective Evolutionary Algorithm with Two Archive and Recombination (TriMOEA_TA&R) strategy [27] benefits those MMMOPs where a subspace can be extracted from the convergence-related decision variables [27]. It also proposed the notion of differential treatment for diversity in decision and in objective space. Two recent studies: Differential Evolution based algorithm for MMMOPs (DE-TriM) [8] and Multi-Modal Neighborhood sensitive Archived Evolutionary Multi-Objective optimizer (MM-NAEMO) [28], use reference vector assisted decomposition of objective space and adaptive reproduction strategies. However, these MMOEAs have inferior performance in the objective space as compared to the standard MOEAs. Earlier in 2019, a Niching Indicator based Multi-Modal Many-Objective optimizer (NIMMO) [29] demonstrated its performance on a few Multi-Modal Many-Objective Problems (MMMaOPs). However, NIMMO [29] investigated its performance only on MMMaOPs [30] with 2-dimensional decision space.

Thus, several MMOEAs [23, 28, 21, 24] exhibit poor convergence and diversity in the objective space and have been tested only on non-scalable problems (with small values of N , M or k_{PS}), which motivate further design of better MMOEAs for problems with high number of variables (N), objectives (M) and subsets of PS (k_{PS}).

¹In this article, decision space, variable space and solution space are considered as synonymous.

The framework proposed in this article is called graph Laplacian based Optimization using Reference vector assisted Decomposition (LORD) and is used for MMMOPs. It is further extended to LORD-II for MMMaOPs. This paper identifies the crowding illusion problem originating from using crowding distance globally over the entire decision space. To reduce its adverse effects, graph Laplacian based clustering (spectral clustering) is used to decompose the decision space while reference vector based approach is used to decompose the objective space. Diversity preservation is conducted in each decomposed sub-region in a collaborative manner. This divide-and-conquer approach uses adaptive hyper-parameters which make the proposed frameworks adaptive to problem characteristics. Performance analysis with the proposed frameworks using the test functions from CEC 2019 competition MMMOPs [4] and polygon problems [30] establish their efficacy.

In the rest of the paper, Section 2 mentions the motivation behind the proposed work, Section 3 outlines the proposed evolutionary frameworks, Section 4 presents the experiments to establish their efficacy and Section 5 concludes the article with scope of future work in this direction.

2 Motivation for the proposed approach

This section illustrates the crowding illusion problem and discusses a few observations which motivates the design of the proposed approach.

2.1 Crowding illusion problem

Most MMMOEAs [18, 21, 23, 8, 22, 20] use CDX to assess the solution distribution. However, using CDX over the entire decision space can be illusional. To describe this issue, let the example in Fig. 2 be considered. It has an isolated ■ solution in the estimated PS. However, due to overlap along different dimensions of the decision space, ■ has nearby neighbors in both objective and decision space impacting the evaluation of CDX and CDF (perimeter of hyper-rectangle bounded by neighbors [23, 8, 18, 21]). Thus, by the crowding distance-based sorting approach of [23, 8, 18, 21], this ■ solution appears towards at the end of the sorted list as a more crowded solution. This ambiguity arising due to the use of CDX globally over the entire decision space is being termed as the crowding illusion problem, henceforth.

2.2 Observations which motivate the design of the proposed approach

The following aspects motivate the design of LORD and LORD-II:

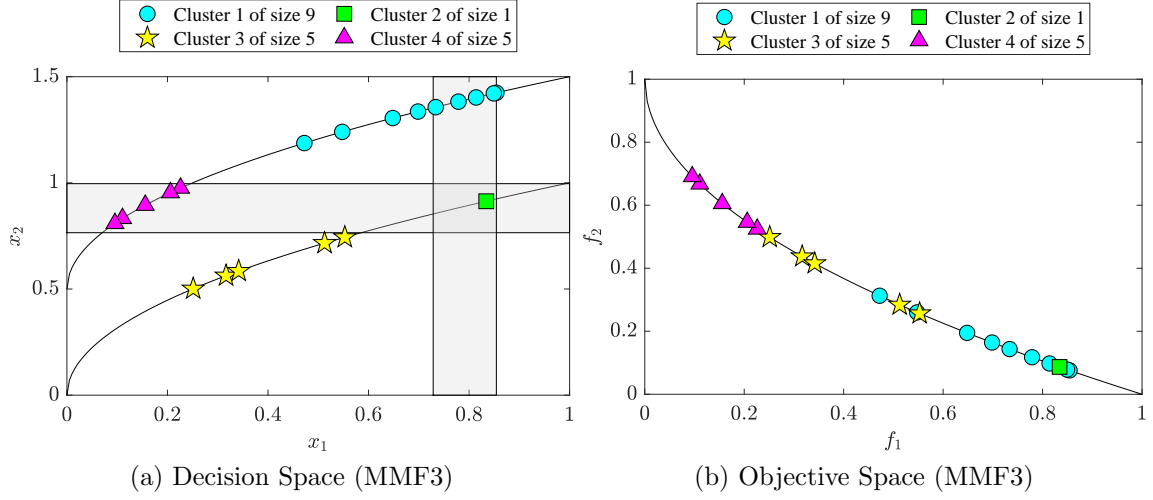


Figure 2: Crowding illusion problem in a benchmark test problem (MMF3 [4]) arises due to overlap along different dimensions of the decision space which gives the illusion that ■ is crowded. Usual sorting of solutions from least crowded to most crowded generates ▲●●●★●▲★●●●●●●●■● (with ■ solution in 19th position) whereas LORD’s sorting generates ●■★▲●★●▲●★▲●●●●●●● (with ■ solution in 2nd position).

1. As there is no established formulation for the solution diversity in the decision space, it is either denoted by the solution distribution [23, 8] or by the number of optimal solutions [27]. Thus, LORD and LORD-II characterize the solution diversity in the decision space using both the number and distribution of solutions.
2. To reduce the effect of the crowding illusion problem (Section 2.1), LORD clusters a set of non-dominated solutions and, then, computes crowding distance within each cluster. For the example in Fig. 2, the ■ solution appears as a much less crowded solution by using this sorting approach.
3. To yield competitive performance in objective space as the standard MOEAs, unlike other MMMOEAs, LORD demonstrates the synergism of diversity preservation, adaptation of hyper-parameters, reference-vector based decomposition of the objective space, and utilization of the neighborhood property [31] during mating pool formation and candidate selection.

To the best of the authors’ knowledge, the proposed work is the first of its kind to use graph Laplacian (a decomposition strategy) in the decision space along with

reference vector assisted decomposition of objective space for handling MMMOPs. Moreover, the proposed framework is also the first to study its scalability on problems in terms of N , M and k_{PS} . Herein, lies the novelty of the proposed work.

3 Proposed Algorithmic Framework

This section outlines the overall framework of LORD while highlighting the major contributions in the population filtering step (line 8 of Algorithm 1).

3.1 General Framework

The overall framework is described in terms of the following features:

Input and Output:

LORD (Algorithm 1) considers the problem description ($prob(N, M)$), population size (n_{pop}), maximum function evaluations ($MaxFES$) and the set of reference-vectors (\mathcal{W} satisfying Eq. (3) to decompose the objective space) as input. It estimates PS and PF as the output. For reference vector assisted decomposition of the objective space, Das and Dennis's approach [16, 31] is used. Its major blocks are outlined next.

$$\mathcal{W} = [\mathbf{W}_1, \mathbf{W}_2, \dots, \mathbf{W}_{n_{dir}}]^T, \quad (3)$$

where $\mathbf{W}_i = [w_{i1}, w_{i2}, \dots, w_{iM}]$ and $\sum_{j=1}^M w_{ij} = 1$, for $i = 1$ to n_{dir}

Initialization:

During initialization (line 2), the population ($\mathcal{A}_{G=1}$) is formed with n_{pop} candidates randomly scattered over \mathcal{D} using Eq. (4).

$$\mathcal{A}_{G=1} = [\mathbf{X}_1, \dots, \mathbf{X}_{n_{pop}}]^T, \text{ where } \mathbf{X}_i = [x_{i1}, \dots, x_{iN}] \quad (4)$$

and $x_{ij} = x_j^L + rand(0, 1) \times (x_j^U - x_j^L)$ for $j = 1, \dots, N$

The mean values of reproduction parameters ($F_{m,G=1}^{DE}$, $CR_{m,G=1}$ and $\eta_{cm,G=1}$) are initialized. For the k^{th} reference vector (\mathbf{W}_k), the indices of other reference vectors are stored in the k^{th} row of the neighborhood lookup matrix, $\mathbf{N}_k \in \mathcal{N}$, sorted by distance from \mathbf{W}_k . As \mathbf{W}_k defines a subspace and \mathbf{N}_k points to its neighbors, \mathcal{N} plays a vital role in mating pool formation to promote diversity.

Generations of LORD:

The for-loop (lines 3 to 13) executes different generations of LORD until $G_{max} = \lfloor MaxFES/n_{dir} \rfloor$. Each generation G iterates over all n_{dir} sub-spaces. Within one iteration, solution perturbation (line 6) and population filtering (line 8) are performed,

Algorithm 1 General Framework

Input: $prob(N, M)$: An MMMOP having N -dimensional decision space (lower-bounded by \mathbf{X}^L and upper-bounded by \mathbf{X}^U) and M -dimensional objective space; n_{pop} : Population size; $MaxFES$: Maximal of fitness evaluations; \mathcal{W} : Set of n_{dir} reference vectors (as in [16, 15])

Output: $\mathcal{A}_{G_{max}}$: Final population estimating PS; $\mathcal{A}_{\mathbf{F}, G_{max}}$: Objective vectors $\forall \mathbf{X} \in \mathcal{A}_{G_{max}}$ estimating PF

```

1: procedure LORD( $prob, n_{pop}, MaxFES, \mathcal{W}$ )
2:   Set  $\mathcal{A}_G, \mathcal{N}, F_{m,G}^{DE}, CR_{m,G}, \eta_{cm,G}$ , for  $G = 1$ 
3:   for  $G = 1$  to  $G_{max}$  do
4:      $\mathbf{S}_{F^{DE}} \leftarrow \emptyset, \mathbf{S}_{CR} \leftarrow \emptyset, \mathbf{S}_{\eta_c} \leftarrow \emptyset$ 
5:     for  $k = 1$  to  $n_{dir}$  (for each direction) do
6:        $[\mathbf{X}_{child}, \mathbf{X}_1, F^{DE}, CR, \eta_c] \leftarrow \text{PERTURB}(\mathcal{A}_G,$ 
          $\mathbf{N}_k, F_{m,G}^{DE}, CR_{m,G}, \eta_{cm,G}, \mathbf{W}_k, P_{mut})$ 
7:       if  $\mathbf{X}_1 \neq \mathbf{X}_{child}$  then
8:          $\mathcal{A}_G \leftarrow \text{FILTER}(\mathcal{A}_G, \mathbf{X}_{child})$ 
9:         if  $\mathbf{X}_{child} \in \mathcal{A}_G$  then
10:           $\mathbf{S}_{F^{DE}} \leftarrow \mathbf{S}_{F^{DE}} \cup F^{DE}, \mathbf{S}_{CR} \leftarrow \mathbf{S}_{CR} \cup CR, \mathbf{S}_{\eta_c} \leftarrow \mathbf{S}_{\eta_c} \cup \eta_c$ 
11:        end if
12:      end if
13:    end for
14:     $F_{m,G+1}^{DE} \leftarrow \text{mean}(\mathbf{S}_{F^{DE}}),$ 
       $CR_{m,G+1} \leftarrow \text{mean}(\mathbf{S}_{CR}),$ 
       $\eta_{cm,G+1} \leftarrow \text{mean}(\mathbf{S}_{\eta_c})$ 
15:  end for
16:  return  $\mathcal{A}_{G_{max}}$  and  $\mathcal{A}_{\mathbf{F}, G_{max}} = \{\mathbf{F}(\mathbf{X}) | \mathbf{X} \in \mathcal{A}_{G_{max}}\}$ 
17: end procedure

```

as described in the next paragraphs. If the child candidate \mathbf{X}_{child} survives the filtering step, the reproduction parameters involved in its creation are appended to respective success vectors ($\mathbf{S}_{F^{DE}}$, \mathbf{S}_{CR} and \mathbf{S}_{η_c}) in steps 9 to 11. When G ends, the mean of reproduction parameters are updated in line 14 using respective success vectors. The population ($\mathcal{A}_{G_{max}}$) at the end of G_{max} generations estimates the PS and the set $\mathcal{A}_{\mathbf{F}, G_{max}}$ of corresponding objective vectors represents the estimated PF.

Solution Perturbation:

To make LORD adaptive to the local properties of the fitness landscape, probabilistic mutation switching [31, 34] is used. The creation of \mathbf{X}^{child} in line 6 of Algorithm 1 uses Algorithm 2. The first parent \mathbf{X}_1 is randomly chosen from the candidates associated with \mathbf{W}_k (line 7). This association is dictated by Eq. (5) where $d2$ is the

Algorithm 2 Reproduction of Child Candidate

Input: \mathcal{A}_G : Population; \mathbf{N}_k : Mating pool; $\{F_{m,G}^{DE}, CR_{m,G}, \eta_{cm,G}\}$: Reproduction parameters; \mathbf{W}_k : k^{th} reference vector; P_{mut} : Probability of mutation switching

Output: \mathbf{X}_{child} : Child; $\{F^{DE}, CR, \eta_c\}$: Reproduction parameters used

```
1: procedure PERTURB( $\mathcal{A}_G, \mathbf{N}_k, F_{m,G}^{DE}, CR_{m,G}, \eta_{cm,G}, \mathbf{W}_k, P_{mut}$ )
2:   if no candidate is associated with  $\mathbf{W}_k$  then
3:      $\mathbf{N}' \leftarrow$  First  $k_{nbr}$  non-empty vectors from  $\mathbf{N}_k$ 
4:      $\mathbf{W}_r \leftarrow$  Reference vector for random index  $r \in \mathbf{N}'$ 
5:      $\mathbf{X}_1 \leftarrow$  Random candidate associated with  $\mathbf{W}_r$ 
6:   else
7:      $\mathbf{X}_1 \leftarrow$  Random candidate associated with  $\mathbf{W}_k$ 
8:   end if
9:   if  $\text{rand}(0, 1) < P_{mut}$  then
10:     $\mathcal{A}_{k,G}^{mat} \leftarrow \text{MATING\_POOL}(\mathbf{N}_k, \mathcal{A}_G, 1)$ 
11:     $\eta_c \leftarrow N(\eta_{cm,G}, 5)$ 
12:     $\mathbf{X}_2 \leftarrow$  Randomly from  $\mathcal{A}_{k,G}^{mat}$ 
13:     $\mathbf{X}'_{child} \leftarrow$  SBX-crossover [14] with  $\mathbf{X}_1, \mathbf{X}_2, \eta_c$ 
14:     $\mathbf{X}_{child} \leftarrow$  Polynomial mutation [32] on  $\mathbf{X}'_{child}$ 
15:     $F^{DE} \leftarrow \emptyset, CR \leftarrow \emptyset$ 
16:   else
17:     $\mathcal{A}_{k,G}^{mat} \leftarrow \text{MATING\_POOL}(\mathbf{N}_k, \mathcal{A}_G, 3)$ 
18:     $F^{DE} \leftarrow N(F_{m,G}^{DE}, 0.1), CR \leftarrow N(CR_{m,G}, 0.1)$ 
19:     $[\mathbf{X}_2, \mathbf{X}_3, \mathbf{X}_4] \leftarrow$  Randomly from  $\mathcal{A}_{k,G}^{mat}$ 
20:     $\mathbf{X}'_{child} \leftarrow \text{DE/rand/1/bin}$  [33] with  $\mathbf{X}_1$  to  $\mathbf{X}_4, F^{DE}, CR$ 
21:     $\mathbf{X}_{child} \leftarrow$  Polynomial mutation [32] on  $\mathbf{X}'_{child}$ 
22:     $\eta_c \leftarrow \emptyset$ 
23:   end if
24:   return  $\mathbf{X}_{child}, \mathbf{X}_1, F^{DE}, CR, \eta_c$ 
25: end procedure
```

minimum perpendicular distance from $\mathbf{F}(\mathbf{X})$ to \mathbf{W}_k .

$$\begin{aligned} \text{Sub-space associated to } \mathbf{W}_k : \{ \mathbf{F}(\mathbf{X}) \in \mathbb{R}^M \mid d2(\mathbf{X}|\mathbf{W}_k) \leq d2(\mathbf{X}|\mathbf{W}_j) \}, \\ \text{for } j = \{1, 2, \dots, n_{dir}\}, k \neq j \text{ and } \mathbf{X} \in \mathcal{D}. \end{aligned} \quad (5)$$

The other remaining parents (in line 10 or 17) and also \mathbf{X}_1 (if the k^{th} sub-space is empty in lines 3 to 5) are randomly chosen using the mating pool ($\mathcal{A}_{k,G}^{mat}$) formation principle (elaborated in next paragraph). The parameter P_{mut} decides between DE/rand/1/bin [35, 33] or SBX crossover [14, 21] (in line 9 or 16). The reproduction

Algorithm 3 Mating Pool Formation

Input: \mathbf{N}_k : Sorted array of nearest neighboring directions of \mathbf{W}_k ; \mathcal{A}_G : Population in decision space; n_S : Number of sub-spaces to be chosen

Output: $\mathcal{A}_{k,G}^{mat}$: Sub-population selected for mating

- 1: **procedure** MATING_POOL($\mathbf{N}_k, \mathcal{A}_G, n_S$)
 - 2: $\mathbf{N}' \leftarrow$ First k_{nbr} non-empty vectors from \mathbf{N}_k
 - 3: $\{\mathbf{W}_{r_1}, \dots, \mathbf{W}_{r_{n_S}}\} \leftarrow$ Reference vectors for random indices
 $\{r_1, \dots, r_{n_S}\} \in \mathbf{N}'$
 - 4: $\mathcal{A}_{k,G}^{mat} \leftarrow$ Candidates of \mathcal{A}_G associated with $\{\mathbf{W}_{r_1}, \dots, \mathbf{W}_{r_{n_S}}\}$
 - 5: **return** $\mathcal{A}_{k,G}^{mat}$
 - 6: **end procedure**
-

parameters (η_c , F^{DE} and CR) are sampled from Gaussian distributions [36, 31] with mean values provided by $\eta_{cm,G}$, $F_{m,G}^{DE}$ and $CR_{m,G}$. The standard deviations of the distributions are varied in the range $[0.05, 0.2]$ for F^{DE} and CR and $[1, 6]$ for η_c and the best-performing values are specified in lines 11 and 18. For SBX crossover, one of two children is randomly considered (in line 13). Both SBX crossover and DE/rand/1/bin are followed by polynomial mutation [32] in lines 14 and 21, respectively, as it helps to avoid local optima [32]. The child candidate (\mathbf{X}_{child}), the parent candidate (\mathbf{X}_1) and the sampled values of reproduction parameters are returned in line 24. Depending on the choice of if-condition in line 9 of Algorithm 2, either η_c or F^{DE} and CR are empty so only used values of reproduction parameters are appended to the success vectors in line 10 of Algorithm 1.

Mating Pool Formation:

The idea is to leverage the neighborhood property [31] for a uniform exploration, i.e., higher chances of \mathbf{X}^{child} creation in an unexplored subspace occurs if candidates from its neighboring regions participate in mating [31, 15]. The mating pool ($\mathcal{A}_{k,G}^{mat}$) formation in line 10 or 17 of Algorithm 2 uses Algorithm 3. It considers k_{nbr} nearest non-empty reference vectors of \mathbf{W}_k (line 2), from which n_S random reference vectors $\{\mathbf{W}_{r_1}, \dots, \mathbf{W}_{r_{n_S}}\}$ are selected in line 3. The parameter n_S is the minimum number of additional parents required as per a reproduction strategy (3 for DE/rand/1/bin and 1 for SBX crossover). All candidates associated with $\{\mathbf{W}_{r_1}, \dots, \mathbf{W}_{r_{n_S}}\}$ form $\mathcal{A}_{k,G}^{mat}$ in line 4 and returned from line 5. For association, Eq. (5) is considered as done in [15, 14].

Population Filtering:

If \mathbf{X}_{child} is better than its parent (\mathbf{X}_1), to maintain a constant n_{pop} , one of the candidates from $\mathcal{A}_G \cup \mathbf{X}^{child}$ is removed in line 8 of Algorithm 1 by calling the filtering operation, which is described after explaining the approach to decompose the population in the decision space.

3.2 Decomposition of the Decision Space

The filtering step in line 8 of Algorithm 1 involves graph Laplacian based partitioning [37, 38] of a set of solutions (\mathcal{A}^{nd}) in the decision space. This graph partitioning helps in picking up solutions from each cluster to yield a balanced solution set and to reduce the effect of crowding illusion during diversity estimation. Spectral graph theory is associated with studying properties of a graph using eigen decomposition of its Laplacian matrix representation [37, 38]. These properties assist in the spectral clustering of \mathcal{A}^{nd} through the following steps:

1) *Create nearest neighbor graph (\mathcal{G})*: All candidates of \mathcal{A}^{nd} are used as the nodes of graph \mathcal{G} . Euclidean distances between all pairs of candidates in \mathcal{A}^{nd} are evaluated. Edges are placed between pairs of candidates (nodes) where distance is less than a threshold of ε_L . Specifically, \mathcal{G} (binary symmetric matrix) is the adjacency matrix representation.

2) *Obtain symmetric normalized graph Laplacian (\mathcal{L}_{sym})*: A diagonal matrix \mathcal{G}_d is created using the degree of each node (row sum) of \mathcal{G} . Using the identity matrix I of the same order as \mathcal{G} and \mathcal{G}_d , \mathcal{L}_{sym} [37] is obtained by Eq. (6).

$$\mathcal{L}_{sym} = I - \mathcal{G}_d^{-1/2} \mathcal{G} \mathcal{G}_d^{-1/2} \quad (6)$$

3) *Obtain number of connected components (k_{CC})*: The algebraic multiplicity of 0 eigen value of \mathcal{L}_{sym} [37, 38] gives the number of connected components (k_{CC}) of \mathcal{G} .

4) *Assign candidates (nodes) to k_{CC} clusters*: By Cheeger's inequality [39, 40], the sparsest cut of a graph is approximated by the second smallest eigenvalue of \mathcal{L}_{sym} . Thus, all the eigen vectors from the second smallest to the k_{CC}^{th} eigenvalues are clustered ($\mathcal{C}_1, \dots, \mathcal{C}_{k_{CC}}$) using k-means [41] for assigning the candidates of \mathcal{A}^{nd} to the clusters (partitions) in the decision space. An example of spectral clustering a non-dominated set of solutions is illustrated in Fig. 2a for a benchmark test problem (MMF3) [4].

For reducing crowding illusion (Section 2.1), spectral clustering of \mathcal{A}^{nd} is chosen over k-means clustering due to the following reasons: (1) k-means is effective only for globular structures whereas spectral clustering is effective for non-globular structure as well [42] (a comparison is provided in Section 5 of the supplementary material at <https://worksupplements.droppages.com/lord>), (2) k_{CC} for k-means is not known apriori whereas k_{CC} for spectral clustering can be obtained mathematically and (3) k-means (performed in the step 4 of spectral clustering of \mathcal{A}^{nd}) becomes independent of the number of decision variables (N).

Algorithm 4 Filter for constant Population Size (LORD)

Input: \mathcal{A}_G : Current population; \mathbf{X}_{child} : Child candidate

Output: \mathcal{A}_G : Filtered population of size n_{pop} ;

```

1: procedure FILTER( $\mathcal{A}_G, \mathbf{X}_{child}$ )
2:    $\mathcal{A}_{F,G}^{all} = \{\mathbf{F}(\mathbf{X}) | \mathbf{X} \in (\mathcal{A}_G \cup \mathbf{X}_{child})\}$ 
3:    $\mathcal{A}_F^{nd} \leftarrow$  Last non-dominated rank of  $\mathcal{A}_{F,G}^{all}$ 
4:    $\mathcal{A}^{nd} = \{\mathbf{X} | \mathbf{F}(\mathbf{X}) \in \mathcal{A}_F^{nd}\}$ 
5:    $\{\mathcal{C}_1, \dots, \mathcal{C}_{k_{cc}}\} \leftarrow$  Spectral clustering of  $\mathcal{A}^{nd}$ 
6:   Evaluate SCD cluster-wise
7:    $\mathcal{A}_s^{nd} \leftarrow$  Select one-by-one from  $\mathcal{C}_1$  to  $\mathcal{C}_{k_{cc}}$  w.r.t. SCD
8:   for  $j = |\mathcal{A}_s^{nd}|$  to 1 (starting from most-crowded) do
9:      $\mathbf{W}_k \leftarrow$  Direction where  $\mathbf{X}_j \in \mathcal{A}_s^{nd}$  is associated
10:    if #candidates associated with  $\mathbf{W}_k > 1$  then
11:       $\mathbf{X}_{del} \leftarrow$  Assign  $\mathbf{X}_j$  for deletion
12:      Break loop
13:    end if
14:  end for
15:  if no  $\mathbf{X}_{del}$  is chosen then
16:     $\mathbf{X}_{del} \leftarrow$  Last candidate of  $\mathcal{A}_s^{nd}$ 
17:  end if
18:   $\mathcal{A}_G \leftarrow (\mathcal{A}_G \cup \mathbf{X}_{child}) - \mathbf{X}_{del}$ 
19:  return  $\mathcal{A}_G$ 
20: end procedure
  
```

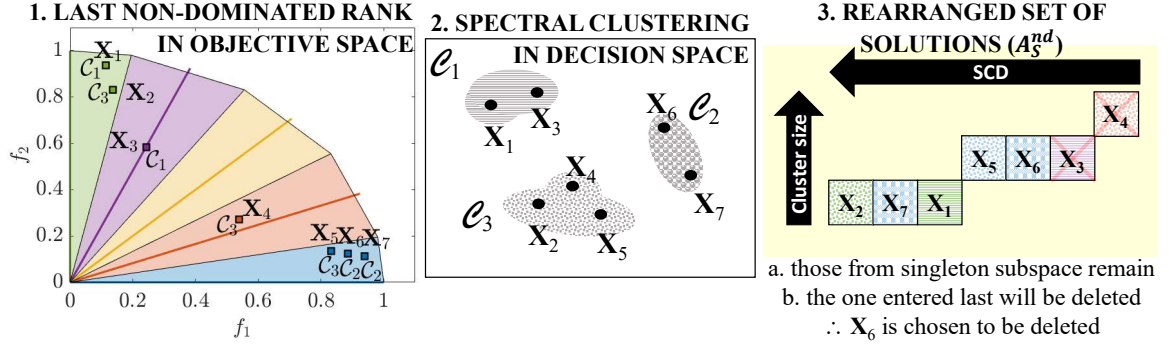


Figure 3: Filtering scheme of LORD on the last non-dominated rank (\mathcal{A}^{nd}).

3.3 Filtering Scheme of LORD framework

The filtering steps of the LORD framework (Algorithm 4) consists of three major steps as follows:

1. *Obtain last non-dominated rank (maintaining convergence in objective space):* Using non-dominated sorting on $(\mathcal{A}_G \cup \mathbf{X}_{child})$, the solutions (\mathcal{A}^{nd}) in the last non-dominated rank [15, 43] are obtained in lines 3 to 4. If $|\mathcal{A}^{nd}| = 1$, lines 5 to 17 yield the only $\mathbf{X}_{del} \in \mathcal{A}^{nd}$ for elimination. Otherwise, some $\mathbf{X}_{del} \in \mathcal{A}^{nd}$ (i.e., from the least converged set of mutually non-dominated candidates) is eliminated by the next steps.
2. *Spectral clustering of candidates from \mathcal{A}^{nd} (maintaining diversity in decision space):* The candidates in \mathcal{A}^{nd} is partitioned in line 5 using the steps mentioned in Section 3.2 as shown in Fig. 3. Evaluating the crowding in the respective spaces, Special Crowding Distance (SCD) [23, 8] combines CDF and CDX. SCD is evaluated per cluster in line 6. A sorted set (\mathcal{A}_s^{nd}) of candidates is formed by rearranging \mathcal{A}^{nd} in line 7 where at first the candidates with the highest SCD is selected from each cluster (e.g., $\mathbf{X}_2 \in \mathcal{C}_3$, $\mathbf{X}_7 \in \mathcal{C}_2$ and $\mathbf{X}_1 \in \mathcal{C}_1$ in Fig. 3), then candidates with the second-highest SCD is selected from each cluster (e.g., $\mathbf{X}_5 \in \mathcal{C}_3$, $\mathbf{X}_6 \in \mathcal{C}_2$ and $\mathbf{X}_3 \in \mathcal{C}_1$ in Fig. 3) and so on (e.g., finally $\mathbf{X}_4 \in \mathcal{C}_3$).
3. *Association based elimination of candidate from \mathcal{A}_s^{nd} (maintaining diversity in objective space):* Starting from the worst candidate (e.g., \mathbf{X}_4) in \mathcal{A}_s^{nd} , the reference vector \mathbf{W}_k is obtained in line 9 with which $\mathbf{X}_j \in \mathcal{A}_s^{nd}$ is associated. If multiple candidates of $(\mathcal{A}_G \cup \mathbf{X}_{child})$ are associated with \mathbf{W}_k (implying a dense sub-space), $\mathbf{X}_{del} = \mathbf{X}_j$ is chosen for deletion (lines 10 to 13). But if the associated sub-space is singleton, \mathbf{X}_j is retained (e.g., \mathbf{X}_4 and \mathbf{X}_3 are retained and $\mathbf{X}_{del} = \mathbf{X}_6$ will be deleted in Fig. 3). If all the sub-spaces with which candidates of \mathcal{A}_s^{nd} are associated are singleton, the last candidate from \mathcal{A}_s^{nd} is chosen for deletion (lines 15 to 17). \mathbf{X}_{del} is deleted from $(\mathcal{A}_G \cup \mathbf{X}_{child})$ in line 18 to yield the filtered \mathcal{A}_G for the next iteration. This filtered \mathcal{A}_G is returned from line 19 of Algorithm 4 to line 8 of main framework (Algorithm 1).

Explicit maintenance of the three essential properties is the most important characteristics of LORD as a novel MMMOEA. While SCD explicitly accounts for solution distribution in decision space, the candidates towards the end of \mathcal{A}_s^{nd} come from the larger clusters (e.g., Fig. 2 and Fig. 3) and are more likely to be deleted. Hence, LORD implicitly takes care of the neighborhood count also as a diversity criterion. This general framework (Algorithm 1) with the filtering scheme in Algorithm 4 is called graph Laplacian based Optimization using Reference vector assisted Decomposition (LORD) whose performance is assessed in Section 4.

Algorithm 5 Filter for constant Population Size (LORD-II)

Input: \mathcal{A}_G : Current population; \mathbf{X}_{child} : Child candidate

Output: \mathcal{A}_G : Filtered population of size n_{pop} ;

```
1: procedure FILTER( $\mathcal{A}_G, \mathbf{X}_{child}$ )
2:    $\mathcal{A}^{nd} \leftarrow \mathcal{A}_G \cup \mathbf{X}_{child}$ 
3:    $\mathcal{A}_{\mathbf{F},G}^{nd} = \{\mathbf{F}(\mathbf{X}) | \mathbf{X} \in \mathcal{A}^{nd}\}$ 
4:    $\mathcal{A}_{del} \leftarrow \emptyset$ 
5:   for  $k = 1$  to  $n_{dir}$  (for each direction) do
6:      $\mathcal{A}_{\mathbf{F},k}^{sub} \leftarrow$  Candidates of  $\mathcal{A}_{\mathbf{F},G}^{nd}$  associated with  $\mathbf{W}_k$ 
7:     if  $|\mathcal{A}_{\mathbf{F},k}^{sub}| > 1$  then
8:        $\mathcal{A}_{del} \leftarrow \mathcal{A}_{del} \cup (\mathbf{X} \text{ with max PBI in } \mathcal{A}_{\mathbf{F},k}^{sub})$ 
9:     end if
10:  end for
11:   $[\mathcal{C}_1, \dots, \mathcal{C}_{k_{CC}}] \leftarrow$  Spectral clustering of  $\mathcal{A}^{nd}$ 
12:   $I_{del} = 0, M_{del} = 0$ 
13:  for  $j = 1$  to  $k_{CC}$  (for all clusters) do
14:    if  $\mathcal{A}_{del} \cap \mathcal{C}_j \neq \emptyset$  then
15:      if  $M_{del} < |\mathcal{C}_j|$  then
16:         $I_{del} = j, M_{del} = |\mathcal{C}_j|$ 
17:      end if
18:    end if
19:  end for
20:   $\mathcal{A}_{del}'' \leftarrow \mathcal{C}_{I_{del}} \cap \mathcal{A}_{del}$ 
21:   $\mathbf{X}_{del} \leftarrow$  Select candidate with max PBI from  $\mathcal{A}_{del}''$ 
22:   $\mathcal{A}_G \leftarrow \mathcal{A}^{nd} - \mathbf{X}_{del}$ 
23:  return  $\mathcal{A}_G$ 
24: end procedure
```

3.4 Filtering Scheme of LORD-II framework

With higher number of objectives, Pareto-dominance fails to provide the necessary selection pressure [1, 2]. Thus, another filtering scheme is presented in Algorithm 5 for which convergence is driven by Penalty-based Boundary Intersection (PBI) instead of Pareto-dominance. As PBI based comparisons are specific to each sub-space, it can efficiently provide the necessary selection pressure. This scheme consists of the following steps:

1. *PBI-based selection for deletion (maintaining convergence in objective space):*
The objective vectors corresponding to all candidates of \mathcal{A}_G and \mathbf{X}_{child} are stored in $\mathcal{A}_{\mathbf{F},G}^{nd}$ in line 3. From each direction, the candidate with the maximum PBI

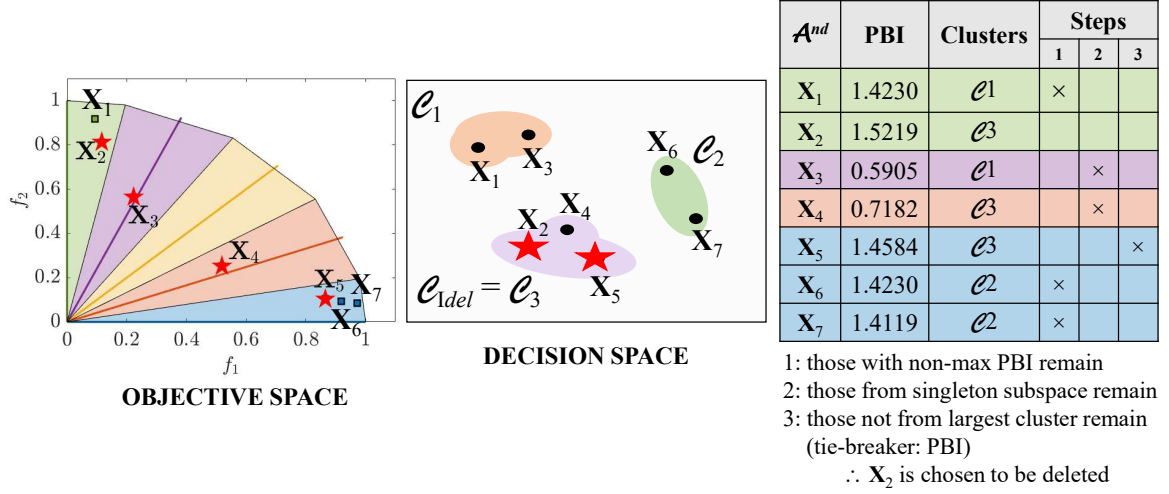


Figure 4: Filtering scheme of LORD-II on a set of solutions (\mathcal{A}^{nd}).

[15, 16, 44] is stored in \mathcal{A}_{del} (lines 4 to 10) as potential candidates for deletion. In Fig. 4, after step 1, $\mathcal{A}_{del} = \{X_2, X_3, X_4, X_5\}$.

2. *Disregarding based on association (maintaining diversity in objective space):* Deletion of a candidate from any sub-space with only one candidate would hamper the diversity in the objective space. Hence, singleton sub-spaces is not considered in \mathcal{A}_{del} (lines 7 to 9). In Fig. 4, after step 2, $\mathcal{A}_{del} = \{X_2, X_5\}$.
3. *Spectral clustering of candidates (maintaining diversity in decision space):* The candidates in \mathcal{A}^{nd} are partitioned in line 11 using the steps mentioned in Section 3.2. The cardinality is noted (lines 12 to 19) only for those clusters which has candidates from the set of potential candidates for deletion \mathcal{A}_{del} (line 14). Then, the candidate (X_{del}) from the largest cluster ($\mathcal{C}_{I_{del}}$), common to \mathcal{A}_{del} , is to be deleted. If multiple such candidates exists (e.g., X_2 and X_5 in Fig. 4), the smaller set \mathcal{A}_{del}'' is formed in line 20. The candidate with the largest PBI in \mathcal{A}_{del}'' is deleted (lines 21 to 22) to yield the filtered \mathcal{A}_G for the next iteration. Thus, in Fig. 4, after step 3, X_2 is deleted.

While the cluster size explicitly accounts for the number of optimal solutions, the spectral clustering implicitly accounts for the solution distribution in the decision space. The general framework (Algorithm 1) with this filtering scheme of Algorithm 5 is called LORD-II.

This combination of the proposed operations allows the LORD and LORD-II to effectively address the two challenges mentioned in Section 1. For the first challenge, graph Laplacian based clustering handles the diversity in the decision space and

reference vector based decomposition handles the diversity in the objective space. The convergence attribute is addressed differently by LORD (using Pareto-dominance) and LORD-II (using PBI based comparisons). For the second challenge, spectral clustering and cluster cardinality helps in obtaining balanced subsets in the PS.

4 Experimental Results

For performance analysis, LORD and LORD-II are implemented in MATLAB R2018a using a 64-bit computer (8 GB RAM, Intel Core i7 @ 2.20 GHz). The experimental specifications of the benchmark MMMOPs, performance measures, and parameter settings of the proposed as well as competitor algorithms are provided in the following sub-sections.

4.1 Benchmark Problems

The benchmark problems from CEC 2019 test suite for MMMOPs [4] are considered with $MaxFES = 5000 \times N$ and $n_{pop} = 100 \times N$, as per [4]. Specifications of these MMMOPS are mentioned in Table 1. It should be noted that MMF12 has discontinuous PF, hence the number of subsets in the global PS (k_{PS}) is one per Pareto-optimal patch. While MMF10-13, MMF15 and MMF15_a have one global PS but these are multi-modal problems as these have local PSs close to their global PS. As MMF14-15, MMF14_a and MMF15_a are scalable in terms of M and N , these are considered as MMMaOPs.

The specifications (p_1 and p_2 divisions in boundary and inside layers, respectively) for defining n_{dir} reference vectors [16, 15] are mentioned in Table 2. The goal is to satisfy $n_{dir} \cong n_{pop} = 100N$.

Performance on the polygon MMMaOPs [30] with $MaxFES = 10000$ are also analyzed using the specifications from [29].

4.2 Performance Indicators

In the objective space, Inverted Generational Distance (IGD) [45] and Hypervolume indicator (HV) [11] are noted for CEC 2019 MMMOPs [4] with $M = 2$ to assess the convergence and diversity of MOEAs [45]. The size of the reference sets² (N_{IGD}) for IGD evaluation and the reference points (\mathbf{R}_{HV}) for HV evaluation are specified in Table 1 as recommended in [4]. For polygon MMMaOPs, IGD with $N_{IGD} = 5000$ is

²Reference sets are obtained from <http://www5.zzu.edu.cn/ecilab/info/1036/1163.htm> for CEC 2019 MMMOPs [4] and from <https://sites.google.com/view/nimmopt/> for polygon MM-MaOPs [30].

Table 1: Specifications for 2-objective MMMOPs in terms of N -dimensional decision space, upper and lower bounded between \mathbf{X}^U and \mathbf{X}^L having reference point at \mathbf{R}_{HV} for HV calculation with N_{IGD} number of points in the reference set for IGD evaluation and number of subsets within PS (k_{PS}).

Problems	N	\mathbf{X}^L	\mathbf{X}^U	\mathbf{R}_{HV}	N_{IGD}	k_{PS}
MMF1	2	$[1, -1]$	$[3, 1]$	$[1.1, 1.1]$	400	2
MMF1_z	2	$[1, -1]$	$[3, 1]$	$[1.1, 1.1]$	400	2
MMF1_e	2	$[1, -20]$	$[3, 20]$	$[1.1, 1.1]$	400	2
MMF2	2	$[0, 0]$	$[1, 1]$	$[1.1, 1.1]$	400	2
MMF3	2	$[0, 0]$	$[1, 1.5]$	$[1.1, 1.1]$	400	2
MMF4	2	$[-1, 0]$	$[1, 2]$	$[1.1, 1.1]$	400	4
MMF5	2	$[1, -1]$	$[3, 3]$	$[1.1, 1.1]$	400	4
MMF6	2	$[1, -1]$	$[3, 2]$	$[1.1, 1.1]$	400	4
MMF7	2	$[1, -1]$	$[3, 1]$	$[1.1, 1.1]$	400	2
MMF8	2	$[-\pi, 0]$	$[\pi, 9]$	$[1.1, 1.1]$	400	4
MMF9	2	$[0.1, 0.1]$	$[1.1, 1.1]$	$[1.21, 11]$	400	2
MMF10	2	$[0.1, 0.1]$	$[1.1, 1.1]$	$[1.21, 13.2]$	400	1
MMF11	2	$[0.1, 0.1]$	$[1.1, 1.1]$	$[1.21, 15.4]$	400	1
MMF12	2	$[0, 0]$	$[1, 1]$	$[1.54, 1.1]$	410	1
MMF13	3	$[0.1, 0.1, 0.1]$	$[1.1, 1.1, 1.1]$	$[1.54, 15.4]$	1250	1
MMF14	$M \geq 3$	$[0, \overset{M}{\cdots}, 0]$	$[1, \overset{M}{\cdots}, 1]$	$[2.2, \overset{M}{\cdots}, 2.2]$	1250	2
MMF14_a	$M \geq 3$	$[0, \overset{M}{\cdots}, 0]$	$[1, \overset{M}{\cdots}, 1]$	$[2.2, \overset{M}{\cdots}, 2.2]$	1250	2
MMF15	$M \geq 3$	$[0, \overset{M}{\cdots}, 0]$	$[1, \overset{M}{\cdots}, 1]$	$[2.5, \overset{M}{\cdots}, 2.5]$	1250	1
MMF15_a	$M \geq 3$	$[0, \overset{M}{\cdots}, 0]$	$[1, \overset{M}{\cdots}, 1]$	$[2.5, \overset{M}{\cdots}, 2.5]$	1250	1
Omni-test	3	$[0, 0, 0]$	$[6, 6, 6]$	$[4.4, 4.4]$	600	27
SYM-PART	2	$[-20, -20]$	$[20, 20]$	$[4.4, 4.4]$	396	9
simple						
SYM-PART	2	$[-20, -20]$	$[20, 20]$	$[4.4, 4.4]$	396	9
rotated						

used as recommended in [29]. Convergence Metric (CM) [46] with the same reference set as IGD and D_metric [47] are used for CEC 2019 MMMOPs [4] with $M \geq 3$ to individually assess the convergence and diversity of MOEAs.

In decision space, IGD [20] and Pareto-Set Proximity (PSP) [23] are used for CEC 2019 MMMOPs [4] with $M = 2$ and for polygon MMMaOPs [30] to assess the performance of MOEAs. For CEC 2019 MMMOPs [4] with $M \geq 3$, the frac-

Table 2: Specifications for reference vector based decomposition for problems with M objectives and N decision variables.

M	p_1	p_2	n_{dir}
2	$100N - 1$	0	$100N$
3	23	0	300
5	8	0	495
8	5	2	828
10	4	3	935

tion of non-contributing solutions³ (NSX) [48, 49] and the convergence metric of this non-contributing set (CM_NSX) are noted. Hereafter, IGDX and IGDF represent IGD values in decision and objective space, respectively, and rHV=1/HV and rPSP=1/PSP are noted such that lower value is the better measure over all the indicators. Brief description of all the performance indicators are provided in Section 2 of the supplementary material.

4.3 Details of Competitor Algorithms

As DN-NSGA-II [21] and MO_Ring_PSO_SCD [23] are MMMOEAs using non-dominated sorting with CDX, LORD is compared with these two MMMOEAs. For comparison with a standard MOEA outperforming the former MMMOEAs in the objective space, LORD is also compared with NSGA-II [2, 50]. For MMMOPs with $M \geq 3$, LORD-II is compared with MO_Ring_PSO_SCD [23] and a popular decomposition based many-objective EA (MOEA/DD) [15].

Other MMMOEAs such as Omni-Optimizer [18], TriMOEA_TA&R [27], MM-NAEMO [28], DE-TriM [8] and NIMMO [29], have demonstrated their effectiveness only for certain kinds of test problems. These MMMOEAs are also compared with LORD and LORD-II on some CEC 2019 MMMOPs [4] and polygon problems [29, 30].

Most of the hyper-parameters of LORD and LORD-II are adaptive in nature, while the rest of them are set as mentioned in Table 3.

4.4 Parameter Sensitivity Studies

Two experiments are presented to study the sensitivity of the following parameters: (1) threshold (ε_L) for nearest neighbor graph formation (Section 3.2), and (2) the probability (P_{mut}) of switching between DE/rand/1/bin and SBX crossover (line 9, Algorithm 2).

³A non-contributing solution is a solution in the non-dominated set whose removal does not change the IGDX of the non-dominated set.

Table 3: Recommended values of different parameters for LORD and LORD-II.

Parameters	Values	Remarks
k_{nbr}	$0.2 \times n_{dir}$	Number of non-empty neighboring directions for mating pool formation (line 2, Algorithm 3) which is easily within $0.2 \times n_{dir}$ as all test cases (except MMF12) have regular PFs
P_{mut}	0.25	Probability of switching among reproduction methods (line 9, Algorithm 2) and sensitivity is analyzed in Section 4.4
ε_L	$\alpha_L \times$ diagonal of \mathcal{D} with $\alpha_L = 0.2$	Threshold on inter-solution distance for formation of nearest neighbor graph (Section 3.2) and sensitivity is analyzed in Section 4.4
$\mu_{F^{DE}, G=1},$ $\mu_{CR, G=1}$ and $\mu_{\eta_c, G=1}$	Initialized as 0.5, 0.2 and 30	Initial mean values of reproduction parameters (line 2, Algorithm 1), later adapted per generation

1. Threshold for Nearest Neighbor Graph: During spectral clustering (Section 3.2) in LORD and LORD-II, the formation of the nearest neighbor graph (\mathcal{G}) considers edges between those pairs of solutions (nodes) whose distance is less than the threshold ε_L . This parameter ε_L is set as α_L ($= 0.2$) times the longest distance in the decision space, i.e., diagonal of the box-constrained decision space, \mathcal{D} . For validating this value of α_L , it is varied between 0.1 to 0.8 (10% to 80% of the diagonal of \mathcal{D}) and the performance of LORD and LORD-II are noted in Table 4 for some MMMOPs with $M = 2$ or $M = 3$.

From Table 4, the best performance is observed when $\alpha_L = 0.2$. The performance deteriorates for higher α_L as all the candidates in \mathcal{A}^{nd} form a single cluster ($k_{CC} = 1$) and distinguishability of the multiple subsets in PS is lost. The performance also deteriorates for lower α_L as $k_{CC} \rightarrow |\mathcal{A}^{nd}|$ and the candidates become independent (higher randomness).

2. Probability of Reproduction Switching: During the probabilistic mutation switching (Algorithm 2) in LORD and LORD-II, P_{mut} decides between DE/rand/1/bin [51] and SBX-crossover [52]. However, in either case, polynomial mutation [32] is also executed. This parameter P_{mut} is set as 0.25 after investigating the following cases:

1. $P_{mut} = 0.00$: only DE/rand/1/bin is used,
2. $P_{mut} = 0.25$: DE/rand/1/bin is used more often than SBX-crossover,

Table 4: Mean IGD_X and IGDF over 51 independent runs for sensitivity study of α_L (parameter of LORD and LORD-II) on some 2- and 3-objective MMMOPs.

	$\alpha_L \rightarrow$	IGDX				IGDF			
		0.1	0.2	0.5	0.8	0.1	0.2	0.5	0.8
LORD	MMF1	0.0504	0.0431	0.0479	0.0492	0.0028	0.0025	0.0025	0.0028
	MMF2	0.1431	0.0180	0.0304	0.0366	0.0092	0.0070	0.0109	0.0173
	MMF3	0.0459	0.0176	0.0419	0.0458	0.0084	0.0069	0.0103	0.0117
	MMF4	0.0298	0.0251	0.0303	0.0352	0.0021	0.0018	0.0023	0.0024
	MMF5	0.0976	0.0814	0.0943	0.1165	0.0025	0.0024	0.0025	0.0027
	MMF6	0.0812	0.0692	0.0720	0.0890	0.0025	0.0023	0.0024	0.0024
	MMF7	0.0277	0.0218	0.0299	0.0339	0.0024	0.0022	0.0026	0.0028
	MMF8	0.1631	0.0762	0.1299	0.1577	0.0025	0.0025	0.0025	0.0025
LORD-II	MMF14	0.0495	0.0443	0.0522	0.0580	0.0550	0.0540	0.0545	0.0546
	MMF14_a	0.0657	0.0576	0.0665	0.0674	0.0574	0.0561	0.0582	0.0583
	MMF15	0.0295	0.0287	0.0292	0.0293	0.0552	0.0548	0.0552	0.0558
	MMF15_a	0.0369	0.0355	0.0373	0.0379	0.0584	0.0571	0.0589	0.0593

3. $P_{mut} = 0.50$: DE/rand/1/bin and SBX-crossover are equally-likely to be used,
4. $P_{mut} = 0.75$: SBX-crossover is used more often than DE/rand/1/bin, and
5. $P_{mut} = 1.00$: only SBX-crossover is used.

The performance of LORD and LORD-II are noted in Table 5 for some MMMOPs. From Table 5, the best performance is observed when $P_{mut} = 0.25$. Hence, for exploration of the search space, DE/rand/1/bin is preferred over SBX-crossover [53] along with a switching scheme to combine the benefits of both these strategies.

Table 5: Mean IGD_X and IGDF over 51 independent runs for sensitivity study of P_{mut} (parameter of LORD and LORD-II) on some 2- and 3-objective MMMOPs.

	$P_{mut} \rightarrow$	IGDX					IGDF				
		0.00	0.25	0.50	0.75	1.00	0.00	0.25	0.50	0.75	1.00
LORD	MMF1	0.0529	0.0431	0.0470	0.0472	0.0506	0.0028	0.0026	0.0027	0.0027	0.0027
	MMF2	0.0694	0.0110	0.0169	0.0207	0.0251	0.0100	0.0069	0.0085	0.0097	0.0141
	MMF3	0.0603	0.0275	0.0116	0.0188	0.0217	0.0169	0.0065	0.0070	0.0082	0.0475
	MMF4	0.0283	0.0237	0.0239	0.0287	0.0381	0.0023	0.0021	0.0021	0.0023	0.0025
	MMF5	0.0923	0.0789	0.0738	0.0900	0.0904	0.0027	0.0025	0.0024	0.0026	0.0028
	MMF6	0.1199	0.0693	0.0777	0.0827	0.0976	0.0025	0.0024	0.0025	0.0025	0.0025
	MMF7	0.0240	0.0209	0.0229	0.0228	0.0278	0.0024	0.0023	0.0023	0.0023	0.0025
	MMF8	0.4619	0.1197	0.1085	0.0737	0.1123	0.0026	0.0025	0.0026	0.0025	0.0026
LORD-II	MMF14	0.0490	0.0484	0.0497	0.0494	0.0502	0.0547	0.0545	0.0542	0.0548	0.0554
	MMF14_a	0.0617	0.0609	0.0613	0.0650	0.0671	0.0578	0.0563	0.0580	0.0589	0.0596
	MMF15	0.0296	0.0288	0.0291	0.0292	0.0291	0.0553	0.0551	0.0552	0.0553	0.0560
	MMF15_a	0.0374	0.0370	0.0364	0.0372	0.0378	0.0588	0.0588	0.0593	0.0594	0.0606

4.5 Comparison of LORD and LORD-II with Other MM-MOEAs

Five sets of experiments are conducted to compare the performance of LORD and LORD-II with other MM-MOEAs.

1) **Experiment-I: Comparison on CEC 2019 Test Suite:** For 2-objective MM-MOPs, the performance of LORD in decision and objective spaces are presented in Tables 6 and 7, respectively. For M -objective MM-MOPs (with $M \geq 3$), the performance of LORD-II is presented in Table 8.

The plots of the estimated PSs and PFs (median run) are presented in Section 3 of the supplementary material. All the results are statistically validated using the Wilcoxon's rank-sum test [48] under the null hypothesis (H_0) that the performance of LORD (or LORD-II) is equivalent to other MM-MOEAs. The statistical significance is indicated using three signs: + denoting LORD (or LORD-II) is superior, - denoting the competitor EA is superior, and \sim indicating the algorithms are equivalent.

From Tables 6 and 7, the following insights are obtained for LORD:

- LORD is superior to DN-NSGA-II [21] as DN-NSGA-II neglects the solution diversity in the objective space. Thus, the solution distribution also suffers in the decision space by the neighborhood property [31].
- While NSGA-II is the second-best in the objective space (Table 7), it neglects the solution diversity in the decision space and thus, gets outperformed by LORD (Table 6).
- While MO_Ring_PSO_SCD is the second-best in the decision space (Table 6), it often gets trapped in the local optima (as seen from estimated PSs and PFs in the supplementary material) leading to poor performance for some MM-MOPs (e.g., MMF11 and MMF12). As LORD efficiently addresses the crowding illusion problem (Section 3.2), it has superior performance in most cases.
- The performance of LORD remains consistent (Tables 6 and 7), even for high k_{PS} (e.g., Omni-test with $k_{PS} = 27$). It can successfully overcome the local optima (e.g., MMF10) and thus, also, acts as an excellent MOEA. The similarity between rPSP ($=IGDX/cov_rate$) and IGDX values imply that cover rate (cov_rate) is nearly equal to one (ideal value) [23].

The following insights can be obtained for LORD-II from Table 8:

- In the objective space (Table 8), both LORD-II and MOEA/DD have similar performance for 3-objective problems. For 5-objective problems, LORD-II

Table 6: Mean \pm Standard Deviation (Significance) of rPSP and IGDX for 2-objective MMMOPs over 51 Runs.

Problems	rPSP=IGDX/cov_rate				IGDX			
	LORD	MO_Ring_PSO_SCD	DN-NSGA-II	NSGA-II	LORD	MO_Ring_PSO_SCD	DN-NSGA-II	NSGA-II
MMF1	0.0441 \pm 0.0044	0.0489 \pm 0.0018 (+)	0.0957 \pm 0.0146 (+)	0.0652 \pm 0.0103 (+)	0.0431 \pm 0.0044	0.0485 \pm 0.0017 (+)	0.0939 \pm 0.0141 (+)	0.0645 \pm 0.0098 (+)
MMF1 _z	0.0356 \pm 0.0069	0.0354 \pm 0.0019 (\sim)	0.0822 \pm 0.0166 (+)	0.3892 \pm 0.3913 (+)	0.0351 \pm 0.0075	0.0352 \pm 0.0018 (\sim)	0.0805 \pm 0.0157 (+)	0.2606 \pm 0.1608 (+)
MMF1 _e	0.8894 \pm 0.1466	0.5501 \pm 0.1276 ($-$)	1.7201 \pm 1.2086 (+)	14.0870 \pm 8.1289 (+)	0.7499 \pm 0.4192	0.4738 \pm 0.0847 ($-$)	1.1536 \pm 0.5095 (+)	3.0324 \pm 0.7634 (+)
MMF2	0.0219 \pm 0.0108	0.0444 \pm 0.0113 (+)	0.1356 \pm 0.0805 (+)	0.0766 \pm 0.0402 (+)	0.0180 \pm 0.0093	0.0416 \pm 0.0103 (+)	0.1121 \pm 0.0525 (+)	0.0650 \pm 0.0300 (+)
MMF3	0.0200 \pm 0.0105	0.0294 \pm 0.0074 (+)	0.1249 \pm 0.1291 (+)	0.0785 \pm 0.0416 (+)	0.0176 \pm 0.0080	0.0276 \pm 0.0061 (+)	0.0968 \pm 0.0632 (+)	0.0661 \pm 0.0311 (+)
MMF4	0.0253 \pm 0.0036	0.0274 \pm 0.0014 (+)	0.0854 \pm 0.0232 (+)	0.1066 \pm 0.0468 (+)	0.0251 \pm 0.0039	0.0271 \pm 0.0014 (+)	0.0849 \pm 0.0230 (+)	0.1004 \pm 0.0411 (+)
MMF5	0.0814 \pm 0.0080	0.0864 \pm 0.0045 (+)	0.1788 \pm 0.0179 (+)	0.1525 \pm 0.0296 (+)	0.0814 \pm 0.0074	0.0857 \pm 0.0044 (+)	0.1763 \pm 0.0165 (+)	0.1478 \pm 0.0265 (+)
MMF6	0.0692 \pm 0.0104	0.0741 \pm 0.0044 (+)	0.1453 \pm 0.0176 (+)	0.1410 \pm 0.0272 (+)	0.0692 \pm 0.0104	0.0736 \pm 0.0042 (+)	0.1433 \pm 0.0173 (+)	0.1372 \pm 0.0251 (+)
MMF7	0.0219 \pm 0.0044	0.0264 \pm 0.0014 (+)	0.0535 \pm 0.0098 (+)	0.0452 \pm 0.0132 (+)	0.0218 \pm 0.0025	0.0262 \pm 0.0014 (+)	0.0524 \pm 0.0092 (+)	0.0420 \pm 0.0106 (+)
MMF8	0.0745 \pm 0.0452	0.0679 \pm 0.0049 (\sim)	0.2969 \pm 0.1120 (+)	0.9348 \pm 0.4682 (+)	0.0762 \pm 0.0504	0.0673 \pm 0.0048 (\sim)	0.2860 \pm 0.1078 (+)	0.7198 \pm 0.3034 (+)
MMF9	0.0047 \pm 0.0002	0.0079 \pm 0.0005 (+)	0.0229 \pm 0.0081 (+)	1.7445 \pm 1.9877 (+)	0.0046 \pm 0.0002	0.0079 \pm 0.0005 (+)	0.0229 \pm 0.0081 (+)	0.1783 \pm 0.0740 (+)
MMF10	0.0018 \pm 0.0007	0.0293 \pm 0.0113 (+)	0.1426 \pm 0.0834 (+)	0.0398 \pm 0.1184 (\sim)	0.0018 \pm 0.0009	0.0276 \pm 0.0092 (+)	0.1295 \pm 0.0747 (+)	0.0398 \pm 0.1184 (\sim)
MMF11	0.0029 \pm 0.0002	0.0055 \pm 0.0003 (+)	0.0045 \pm 0.0003 (+)	0.0027 \pm 0.0003 ($-$)	0.0029 \pm 0.0002	0.0054 \pm 0.0003 (+)	0.0045 \pm 0.0003 (+)	0.0027 \pm 0.0003 ($-$)
MMF12	0.0013 \pm 0.0001	0.0038 \pm 0.0003 (+)	0.0090 \pm 0.0159 (+)	0.0013 \pm 0.0002 (\sim)	0.0013 \pm 0.0001	0.0038 \pm 0.0003 (+)	0.0090 \pm 0.0159 (+)	0.0013 \pm 0.0002 (\sim)
MMF13	0.0243 \pm 0.0039	0.0317 \pm 0.0014 (+)	0.0614 \pm 0.0070 (+)	0.1492 \pm 0.0652 (+)	0.0242 \pm 0.0039	0.0314 \pm 0.0013 (+)	0.0609 \pm 0.0064 (+)	0.0880 \pm 0.0173 (+)
Omni-test	0.0754 \pm 0.0242	0.3946 \pm 0.0939 (+)	1.4390 \pm 0.2069 (+)	1.8176 \pm 0.6886 (+)	0.0706 \pm 0.0215	0.3907 \pm 0.0927 (+)	1.4159 \pm 0.1986 (+)	1.4210 \pm 0.3726 (+)
SYM-PART simple	0.0556 \pm 0.0145	0.1741 \pm 0.0301 (+)	4.1590 \pm 0.8683 (+)	113.0044 \pm 131.2343 (+)	0.0549 \pm 0.0130	0.1733 \pm 0.0300 (+)	4.0657 \pm 0.7040 (+)	6.8332 \pm 1.8906 (+)
SYM-PART rotated	0.1730 \pm 0.0743	0.3142 \pm 0.3533 (+)	5.5941 \pm 3.6017 (+)	13.9239 \pm 12.8588 (+)	0.1558 \pm 0.0760	0.2926 \pm 0.2938 (+)	3.7659 \pm 1.2478 (+)	5.4249 \pm 1.9790 (+)
Sum-up	+/-/ \sim	15/1/2	18/0/0	15/1/2	+/-/ \sim	15/1/2	18/0/0	15/1/2

is marginally outperformed in only one case by MOEA/DD. For 8- and 10-objective problems, LORD-II is superior. In all cases, LORD-II outperforms MO_Ring_PSO_SCD in both convergence (CM) and diversity (D_metric) as also seen in Fig. 6.

- In the decision space (Table 8), LORD-II maintains superiority.
- The estimated PS and PF from LORD-II (Figs. 5 and 6, respectively) demonstrate excellent convergence and diversity. The results from MO_Ring_PSO_SCD deteriorate severely with an increase in dimension. In contrast to MO_Ring_PSO_SCD (Fig. 6d), the polar plot [54] from LORD-II (Fig. 6b) converges all solutions to a near-global PF, forming a uniformly distributed circle for 8-objective MM-MaOPs.

Table 7: Mean \pm Standard Deviation (Significance) of rHV and IGDF for 2-objective MMMOPs over 51 Runs.

Problems	rHV=1/HV				IGDF			
	LORD	MO_Ring_PSO_SCD	DN-NSGA-II	NSGA-II	LORD	MO_Ring_PSO_SCD	DN-NSGA-II	NSGA-II
MMF1	1.0737 \pm 0.0008	1.1484 \pm 0.0005 (+)	1.1495 \pm 0.0014 (+)	1.0738 \pm 0.0006 (\sim)	0.0025 \pm 0.0002	0.0037 \pm 0.0002 (+)	0.0043 \pm 0.0005 (+)	0.0028 \pm 0.0004 (+)
MMF1 _z	1.0731 \pm 0.0008	1.1483 \pm 0.0005 (+)	1.1484 \pm 0.0009 (+)	1.1255 \pm 0.0615 (+)	0.0022 \pm 0.0001	0.0036 \pm 0.0002 (+)	0.0036 \pm 0.0004 (+)	0.0396 \pm 0.0496 (+)
MMF1 _e	1.0751 \pm 0.0021	1.1861 \pm 0.0173 (+)	1.2080 \pm 0.0387 (+)	1.1058 \pm 0.0180 (+)	0.0029 \pm 0.0006	0.0119 \pm 0.0017 (+)	0.0276 \pm 0.0207 (+)	0.0250 \pm 0.0139 (+)
MMF2	1.0817 \pm 0.0120	1.1848 \pm 0.0059 (+)	1.1944 \pm 0.0322 (+)	1.1168 \pm 0.0280 (+)	0.0070 \pm 0.0031	0.0207 \pm 0.0034 (+)	0.0325 \pm 0.0238 (+)	0.0300 \pm 0.0182 (+)
MMF3	1.0792 \pm 0.0322	1.1739 \pm 0.0043 (+)	1.1873 \pm 0.0398 (+)	1.1089 \pm 0.0212 (+)	0.0069 \pm 0.0023	0.0154 \pm 0.0025 (+)	0.0263 \pm 0.0308 (+)	0.0229 \pm 0.0126 (+)
MMF4	1.5234 \pm 0.0003	1.8620 \pm 0.0021 (+)	1.8577 \pm 0.0012 (+)	1.5241 \pm 0.0004 (+)	0.0018 \pm 0.0002	0.0037 \pm 0.0004 (+)	0.0032 \pm 0.0002 (+)	0.0024 \pm 0.0002 (+)
MMF5	1.0734 \pm 0.0006	1.1485 \pm 0.0006 (+)	1.1488 \pm 0.0015 (+)	1.0739 \pm 0.0003 (+)	0.0024 \pm 0.0001	0.0037 \pm 0.0001 (+)	0.0039 \pm 0.0007 (+)	0.0028 \pm 0.0002 (+)
MMF6	1.0732 \pm 0.0003	1.1483 \pm 0.0009 (+)	1.1486 \pm 0.0016 (+)	1.0738 \pm 0.0006 (+)	0.0023 \pm 0.0001	0.0035 \pm 0.0002 (+)	0.0036 \pm 0.0003 (+)	0.0026 \pm 0.0002 (+)
MMF7	1.0731 \pm 0.0002	1.1484 \pm 0.0009 (+)	1.1498 \pm 0.0011 (+)	1.0736 \pm 0.0003 (+)	0.0022 \pm 0.0001	0.0037 \pm 0.0003 (+)	0.0039 \pm 0.0003 (+)	0.0027 \pm 0.0003 (+)
MMF8	1.7915 \pm 0.0012	2.4065 \pm 0.0164 (+)	2.3813 \pm 0.0025 (+)	1.7920 \pm 0.0014 (\sim)	0.0025 \pm 0.0001	0.0048 \pm 0.0002 (+)	0.0040 \pm 0.0004 (+)	0.0025 \pm 0.0001 (\sim)
MMF9	0.0820 \pm 0.0000	0.1034 \pm 0.0000 (+)	0.1034 \pm 0.0000 (+)	0.0820 \pm 0.0000 (\sim)	0.0085 \pm 0.0007	0.0160 \pm 0.0014 (+)	0.0141 \pm 0.0012 (+)	0.0108 \pm 0.0007 (+)
MMF10	0.0678 \pm 0.0000	0.0679 \pm 0.0000 (+)	0.0680 \pm 0.0001 (+)	0.0678 \pm 0.0001 (\sim)	0.0061 \pm 0.0009	0.1128 \pm 0.0230 (+)	0.1446 \pm 0.0660 (+)	0.0074 \pm 0.0000 (+)
MMF11	0.0581 \pm 0.0000	0.0581 \pm 0.0000 (\sim)	0.0581 \pm 0.0000 (\sim)	0.0581 \pm 0.0000 (\sim)	0.0082 \pm 0.0004	0.0176 \pm 0.0018 (+)	0.0136 \pm 0.0014 (+)	0.0107 \pm 0.0008 (+)
MMF12	0.5431 \pm 0.0000	0.5452 \pm 0.0014 (+)	0.5598 \pm 0.0492 (\sim)	0.5430 \pm 0.0000 ($-$)	0.0020 \pm 0.0001	0.0068 \pm 0.0006 (+)	0.0110 \pm 0.0187 (+)	0.0020 \pm 0.0001 (\sim)
MMF13	0.0444 \pm 0.0000	0.0444 \pm 0.0000 (\sim)	0.0444 \pm 0.0000 (\sim)	0.0444 \pm 0.0000 (\sim)	0.0063 \pm 0.0014	0.0264 \pm 0.0076 (+)	0.0121 \pm 0.0036 (+)	0.0089 \pm 0.0014 (+)
Omni-test	0.0518 \pm 0.0000	0.0190 \pm 0.0000 ($-$)	0.0189 \pm 0.0000 ($-$)	0.0518 \pm 0.0000 (\sim)	0.0091 \pm 0.0015	0.0422 \pm 0.0034 (+)	0.0080 \pm 0.0005 ($-$)	0.0100 \pm 0.0021 (\sim)
SYM-PART simple	0.0520 \pm 0.0000	0.0605 \pm 0.0001 (+)	0.0601 \pm 0.0000 (+)	0.0520 \pm 0.0000 (\sim)	0.0165 \pm 0.0039	0.0419 \pm 0.0044 (+)	0.0127 \pm 0.0014 ($-$)	0.0109 \pm 0.0013 ($-$)
SYM-PART rotated	0.0520 \pm 0.0000	0.0606 \pm 0.0001 (+)	0.0601 \pm 0.0000 (+)	0.0520 \pm 0.0000 (\sim)	0.0178 \pm 0.0047	0.0467 \pm 0.0058 (+)	0.0152 \pm 0.0022 ($-$)	0.0159 \pm 0.0040 (\sim)
Sum-up	+/-/ \sim	15/1/2	14/1/3	8/1/9	+/-/ \sim	18/0/0	15/3/0	13/1/4

2) **Experiment-II: Comparison with Reference Vector Assisted MM-MOEAs:** The performance of two recent reference-vector assisted MM-MOEAs (DE-TriM [8] and MM-NAEMO [28]) are compared with LORD and LORD-II in Table 9 on CEC 2019 MMMOPs [4]. The results of this experiment are also compared with MO_Ring_PSO_SCD to fairly assess the relative rankings of algorithms. Each of these algorithms (DE-TriM, MM-NAEMO and MO_Ring_PSO_SCD) are set up using the parameters recommended in [8], [28] and [23], respectively.

From Table 9, LORD-II is noted to have the best performance in all cases and LORD is noted to have the best or the second-best performance in both objective and decision spaces for most of the cases. Unlike other MM-MOEAs [23, 28, 24] which yield poor convergence and/or diversity in objective space in order to improve the performance in decision space, LORD and LORD-II perform satisfactorily in both the

Table 8: Mean \pm Standard Deviation (Significance) of NSX, CM_NSX, D_metric and CM for M -objective ($M \geq 3$) MMMOPs over 51 Runs.

Problems (M)	NSX			CM_NSX			D_metric			CM		
	LORD-II	MO_Ring_ PSO_SCD	MOEA/DD	LORD-II	MO_Ring_ PSO_SCD	MOEA/DD	LORD-II	MO_Ring_ PSO_SCD	MOEA/DD	LORD-II	MO_Ring_ PSO_SCD	MOEA/DD
MMF14 (3)	0.0068 \pm 0.0052	0.2400 \pm 0.0262(+)	0.0133 \pm 0.0024 (+)	0.0203 \pm 0.0018	0.1078 \pm 0.0088 (+)	0.0228 \pm 0.0019 (+)	0.0000 \pm 0.0000	21.3266 \pm 2.0086 (+)	0.0000 \pm 0.0000 (\sim)	0.0419 \pm 0.0003	0.1083 \pm 0.0130 (+)	0.0419 \pm 0.0002 (\sim)
MMF14_a (3)	0.0251 \pm 0.0290	0.2533 \pm 0.0320 (+)	0.1333 \pm 0.0259 (+)	0.1498 \pm 0.0518	0.1534 \pm 0.0147 (+)	0.2481 \pm 0.0103 (+)	0.0000 \pm 0.0000	22.2752 \pm 2.2816 (+)	0.0000 \pm 0.0000 (\sim)	0.0435 \pm 0.0007	0.0949 \pm 0.0149 (+)	0.0438 \pm 0.0010 (\sim)
MMF15 (3)	0.0205 \pm 0.0073	0.4033 \pm 0.0361 (+)	0.0400 \pm 0.0024 (+)	0.0209 \pm 0.0010	0.2356 \pm 0.0251 (+)	0.0265 \pm 0.0039 (\sim)	0.0000 \pm 0.0000	24.4073 \pm 3.8341 (+)	0.0000 \pm 0.0000 (\sim)	0.0422 \pm 0.0004	0.1471 \pm 0.0161 (+)	0.0426 \pm 0.0004 (\sim)
MMF15_a (3)	0.0179 \pm 0.0076	0.3400 \pm 0.0262 (+)	0.0567 \pm 0.0024 (+)	0.0270 \pm 0.0180	0.2069 \pm 0.0263 (+)	0.0454 \pm 0.0098 (+)	0.0000 \pm 0.0000	22.5315 \pm 3.5845(+)	0.0000 \pm 0.0000 (\sim)	0.0445 \pm 0.0007	0.1322 \pm 0.0207 (+)	0.0449 \pm 0.0008 (\sim)
MMF14 (5)	0.4838 \pm 0.0125	0.5140 \pm 0.0168 (+)	0.5152 \pm 0.0057 (+)	0.1830 \pm 0.0015	0.2363 \pm 0.0047 (+)	0.1874 \pm 0.0015 (+)	0.0000 \pm 0.0000	43.9023 \pm 4.6565 (+)	0.0000 \pm 0.0000 (\sim)	0.0590 \pm 0.0020	0.4121 \pm 0.0177 (+)	0.0587 \pm 0.0015 (\sim)
MMF14_a (5)	0.4855 \pm 0.0141	0.4960 \pm 0.0175 (\sim)	0.5232 \pm 0.0029 (+)	0.2080 \pm 0.0155	0.2809 \pm 0.0041 (+)	0.2474 \pm 0.0044 (+)	0.0000 \pm 0.0000	46.7494 \pm 2.8893 (+)	0.9428 \pm 0.8165 (+)	0.0781 \pm 0.0022	0.3659 \pm 0.0115 (+)	0.0827 \pm 0.0021 (+)
MMF15 (5)	0.4959 \pm 0.0076	0.5600 \pm 0.0155 (+)	0.5172 \pm 0.0014 (+)	0.1559 \pm 0.0015	0.4118 \pm 0.0152 (+)	0.1602 \pm 0.0005 (\sim)	0.0000 \pm 0.0000	43.6883 \pm 3.9734 (+)	0.0000 \pm 0.0000 (\sim)	0.0654 \pm 0.0017	0.4610 \pm 0.0152 (+)	0.0625 \pm 0.0025 (\sim)
MMF15_a (5)	0.4969 \pm 0.0086	0.5660 \pm 0.0155 (+)	0.5232 \pm 0.0071 (+)	0.1783 \pm 0.0062	0.3672 \pm 0.0128 (+)	0.1938 \pm 0.0078 (+)	0.0000 \pm 0.0000	45.2327 \pm 3.4695 (+)	0.9428 \pm 0.8165 (+)	0.0954 \pm 0.0045	0.4339 \pm 0.0162 (+)	0.0961 \pm 0.0053 (\sim)
MMF14 (8)	0.2772 \pm 0.0012	0.5663 \pm 0.0129 (+)	0.3088 \pm 0.0018 (+)	0.4025 \pm 0.0011	0.4386 \pm 0.0070 (+)	0.4178 \pm 0.0011 (+)	0.0000 \pm 0.0000	101.1673 \pm 4.3256 (+)	5.3833 \pm 0.0000 (+)	0.1332 \pm 0.0002	0.6277 \pm 0.0154 (+)	0.1456 \pm 0.0016 (+)
MMF14_a (8)	0.2796 \pm 0.0008	0.5588 \pm 0.0114 (+)	0.2900 \pm 0.0062 (+)	0.4222 \pm 0.0004	0.4480 \pm 0.0045 (+)	0.4335 \pm 0.0021 (+)	0.0000 \pm 0.0000	106.8644 \pm 3.5223 (+)	5.3833 \pm 0.0000 (+)	0.1742 \pm 0.0044	0.5917 \pm 0.0149 (+)	0.1817 \pm 0.0044 (+)
MMF15 (8)	0.2524 \pm 0.0002	0.6438 \pm 0.0175 (+)	0.2713 \pm 0.0018 (+)	0.3537 \pm 0.0052	0.5312 \pm 0.0059 (+)	0.3815 \pm 0.0015 (+)	0.0000 \pm 0.0000	99.5550 \pm 3.0343 (+)	5.4810 \pm 0.1382 (+)	0.1288 \pm 0.0038	0.6767 \pm 0.0128 (+)	0.1508 \pm 0.0008 (+)
MMF15_a (8)	0.2430 \pm 0.0137	0.6113 \pm 0.0093 (+)	0.2688 \pm 0.0027 (+)	0.3797 \pm 0.0115	0.4885 \pm 0.0078 (+)	0.3886 \pm 0.0068 (\sim)	0.0000 \pm 0.0000	103.5948 \pm 3.5180 (+)	5.5787 \pm 0.0000 (+)	0.2014 \pm 0.0025	0.6488 \pm 0.0151 (+)	0.2122 \pm 0.0284 (+)
MMF14 (10)	0.2595 \pm 0.0005	0.5880 \pm 0.0101 (+)	0.2620 \pm 0.0038 (+)	0.5088 \pm 0.0087	0.5584 \pm 0.0046 (+)	0.5356 \pm 0.0085 (+)	14.1331 \pm 2.5516	132.4681 \pm 4.6720 (+)	38.9838 \pm 0.7255 (+)	0.2200 \pm 0.0037	0.6575 \pm 0.0129 (+)	0.2504 \pm 0.0002 (+)
MMF14_a (10)	0.2717 \pm 0.0106	0.5930 \pm 0.0134 (+)	0.2718 \pm 0.0083 (\sim)	0.5165 \pm 0.0008	0.5699 \pm 0.0036 (+)	0.5393 \pm 0.0063 (+)	21.9290 \pm 0.4837	137.8081 \pm 3.8224 (+)	41.7357 \pm 0.5083 (+)	0.2554 \pm 0.0065	0.6311 \pm 0.0128 (+)	0.2966 \pm 0.0041 (+)
MMF15 (10)	0.2557 \pm 0.0023	0.6590 \pm 0.0123 (+)	0.2481 \pm 0.0030 (\sim)	0.4516 \pm 0.0096	0.6180 \pm 0.0071 (+)	0.4850 \pm 0.0005 (+)	17.6340 \pm 1.4436	131.8568 \pm 4.0914 (+)	36.4571 \pm 9.3681 (+)	0.2219 \pm 0.0118	0.7072 \pm 0.0109 (+)	0.2535 \pm 0.0072 (+)
MMF15_a (10)	0.2664 \pm 0.0143	0.6350 \pm 0.0119 (+)	0.2652 \pm 0.0098 (\sim)	0.4731 \pm 0.0061	0.5780 \pm 0.0048 (+)	0.4903 \pm 0.0006 (+)	23.2171 \pm 2.4365	133.7104 \pm 2.8705 (+)	39.7423 \pm 1.7614 (+)	0.2672 \pm 0.0037	0.6812 \pm 0.0092 (+)	0.3193 \pm 0.0007 (+)
Sum-up	+/- / \sim	15/0/1	13/1/2	+/- / \sim	16/0/0	13/0/3	+/- / \sim	16/0/0	10/0/6	+/- / \sim	16/0/0	9/1/6

spaces and competitively outperform the other reference vector assisted MMMAEs.

3) **Experiment-III: Comparison on Polygon MMMAEs:** Similar to [29], the mean IGDX and IGDF of LORD-II are compared with NIMMO on Polygon test problems as both the MMMAEs are designed for MMMAEs. The results of MO_Ring_PSO_SCD [23], Omni-Optimizer [18] and TriMOEA_TA&R [27] are also compared.

The performance of these MMMAEs are noted on M -objective polygon and rotated polygon MMMAEs [30] in Tables 11 (using IGDX) and 12 (using IGDF). This experiment considers the specifications mentioned in Table 10 as recommended in [29]. The performance values of the other MMMAEs (except LORD-II) are also noted from [29]. The remaining parameters of LORD-II are set up as specified in Table 3.

From Tables 11 and 12, LORD-II is observed to be superior in both decision and objective spaces, respectively. The performance of all MMMAEs (except TriMOEA_TA&R) are unaffected due to rotation. However, the IGDX values of TriMOEA_TA&R are widely different (poorer) for rotated polygon problems from those of the polygon problems (Table 11). This difference arises as TriMOEA_TA&R considers only the number of solutions as the diversity criteria and neglects the solution

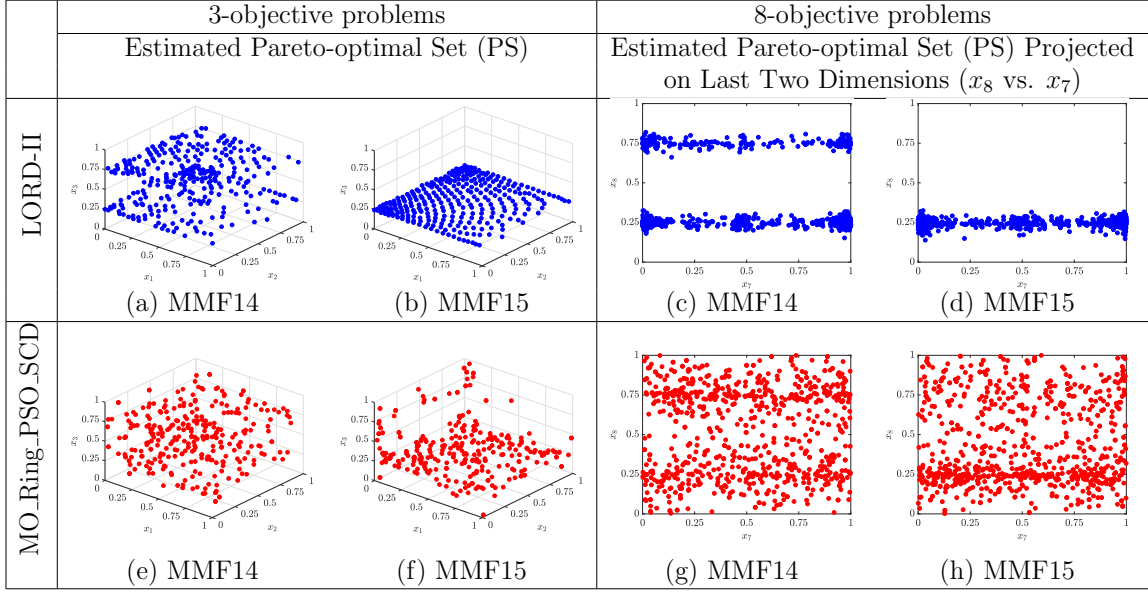


Figure 5: Visualizations of Pareto-optimal Set (PS) 3- and 8-objective MMF14 and MMF15 problems for median runs by LORD-II (top row) and MO_Ring_PSO_SCD (bottom row).

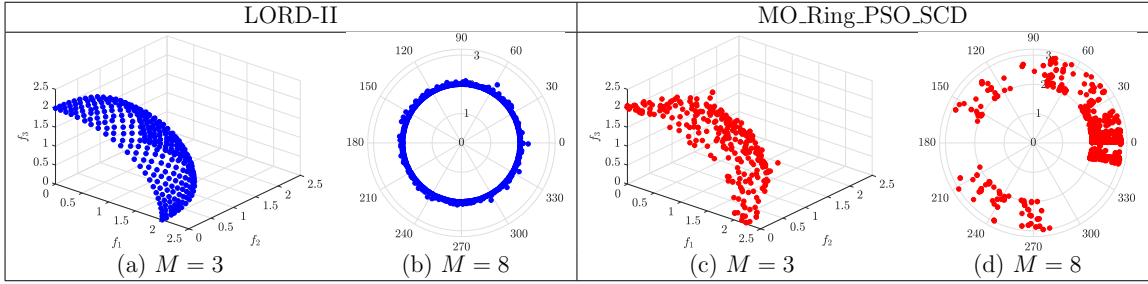


Figure 6: Visualizations of estimated Pareto-Front (PF) of M -objective MMF14 problem for median runs by LORD-II and MO_Ring_PSO_SCD. Results are similar for MMF15 as well.

distribution in the decision space [27].

The estimated PSs from LORD-II are shown in Table 13 from which the following observations are noted:

- For all the 8 instances, LORD-II converges to global surfaces without any outliers.
- The number of solutions per subset is relatively uniform over the 9 subsets in PS.

Table 9: Mean of IGDX and IGDF over 51 independent runs for comparing reference-vector guided MMMOEAs on 2- and 3-objective MMMOPs.

2-objective Problems	IGDX				IGDF			
	LORD	DE-TriM	MM-NAEMO	MO.Ring-PSO_SCD	LORD	DE-TriM	MM-NAEMO	MO.Ring-PSO_SCD
MMF1	0.0431	0.0465 (+)	0.0486 (+)	0.0485 (+)	0.0025	0.0026 (~)	0.0040 (+)	0.0037 (+)
MMF1 _z	0.0351	0.0503 (+)	0.0347 (~)	0.0352 (~)	0.0022	0.0026 (+)	0.0035 (+)	0.0036 (+)
MMF1 _e	0.7499	2.8757 (+)	0.4115 (-)	0.4738 (-)	0.0029	0.0029 (~)	0.0051 (+)	0.0119 (+)
MMF2	0.0180	0.0505 (+)	0.0118 (-)	0.0416 (+)	0.0070	0.0035 (-)	0.0083 (+)	0.0207 (+)
MMF3	0.0176	0.0235 (+)	0.0137 (-)	0.0276 (+)	0.0069	0.0047 (-)	0.0085 (+)	0.0154 (+)
MMF4	0.0251	0.0211 (-)	0.0312 (+)	0.0271 (+)	0.0018	0.0025 (+)	0.0033 (+)	0.0037 (+)
MMF5	0.0814	0.0892 (+)	0.0871 (+)	0.0857 (+)	0.0024	0.0027 (+)	0.0037 (+)	0.0037 (+)
MMF6	0.0692	0.0756 (+)	0.0743 (+)	0.0736 (+)	0.0023	0.0025 (~)	0.0036 (+)	0.0035 (+)
MMF7	0.0218	0.0201 (-)	0.0229 (+)	0.0262 (+)	0.0022	0.0025 (+)	0.0035 (+)	0.0037 (+)
MMF8	0.0762	0.0989 (+)	0.3348 (+)	0.0673 (~)	0.0025	0.0029 (+)	0.0037 (+)	0.0048 (+)
MMF9	0.0046	0.0787 (+)	0.0048 (~)	0.0079 (+)	0.0085	0.0119 (+)	0.0479 (+)	0.0160 (+)
MMF10	0.0018	0.0018 (~)	0.0121 (+)	0.0276 (+)	0.0061	0.0080 (+)	0.0639 (+)	0.1128 (+)
MMF11	0.0029	0.0036 (+)	0.0418 (+)	0.0054 (+)	0.0082	0.0109 (+)	0.0931 (+)	0.0176 (+)
MMF12	0.0013	0.0013 (~)	0.0050 (+)	0.0038 (+)	0.0020	0.0021 (~)	0.0196 (+)	0.0068 (+)
MMF13	0.0242	0.0368 (+)	0.1878 (+)	0.0314 (+)	0.0063	0.0094 (+)	0.1059 (+)	0.0264 (+)
Omni-test	0.0706	0.0732 (+)	0.1511 (+)	0.3907 (+)	0.0091	0.0125 (+)	0.0130 (+)	0.0422 (+)
SYM-PART-simple	0.0549	0.0740 (+)	0.1115 (+)	0.0300 (-)	0.0165	0.0101 (-)	0.0472 (+)	0.0419 (+)
SYM-PART-rotated	0.1558	0.1885 (+)	0.7586 (+)	0.2926 (+)	0.0178	0.0125 (-)	0.0395 (+)	0.0467 (+)
LORD vs. others (+/-/~)		14/2/2	13/3/2	14/2/2	(+/-/~)	10/4/4	18/0/0	18/0/0
3-objective Problems	LORD-II	DE-TriM	MM-NAEMO	MO.Ring-PSO_SCD	LORD-II	DE-TriM	MM-NAEMO	MO.Ring-PSO_SCD
MMF14	0.0443	0.0558 (+)	0.0465 (+)	0.0539 (+)	0.0540	0.0749 (+)	0.0808 (+)	0.0801 (+)
MMF14 _a	0.0576	0.0676 (+)	0.0663 (+)	0.0613 (+)	0.0561	0.0809 (+)	0.0791 (+)	0.0789 (+)
MMF15	0.0287	0.0361 (+)	0.0518 (+)	0.0419 (+)	0.0548	0.0787 (+)	0.1113 (+)	0.0854 (+)
MMF15 _a	0.0355	0.0503 (+)	0.0848 (+)	0.0452 (+)	0.0571	0.0951 (+)	0.1263 (+)	0.0841 (+)
LORD-II vs. others (+/-/~)		4/0/0	4/0/0	4/0/0	(+/-/~)	4/0/0	4/0/0	4/0/0

Table 10: Specifications for the experiment conducted on polygon and rotated polygon problems according to recommendations in [29].

Parameters		Used by LORD-II	Used by NIMMO, TriMOEA-TA&R, MO.Ring-PSO_SCD, and Omni-Optimizer in [29]
n_{pop}	3-obj	210	210
	5-obj	210	210
	8-obj	156	156
	10-obj	210	210
#runs		31	31
$MaxFES$		10000	10000
N_{IGD}		5000	5000

- For both polygon and rotated polygon problems, the shape of the polygon is properly replicated for 3- and 5-objective problems. For 8- and 10-objective problem, a near-spherical blob (of unidentifiable shape) is formed at each of the subsets in PS.

4) **Experiment-IV: Comparison of LORD and LORD-II with CEC 2019 winner:** To deal with the reduced selection pressure of dominance-based filtering

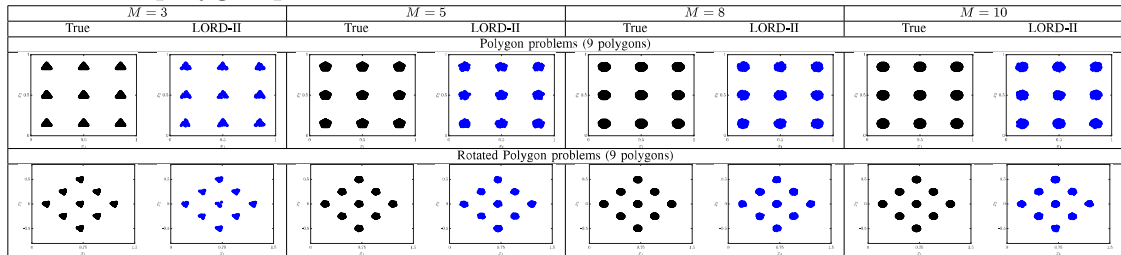
Table 11: Mean IGDX over 31 independent runs for comparing LORD-II on M -objective polygon and rotated polygon (RPolygon) problems.

M -Problems	LORD-II	NIMMO	TriMOEA _TA&R	MO_Ring_ PSO_SCD	Omni- Optimizer
3-Polygon	0.0054	0.0056 (+)	0.0063 (+)	0.0091 (+)	0.0083 (+)
3-RPolygon	0.0064	0.0059 (−)	0.0295 (+)	0.0090 (+)	0.0085 (+)
5-Polygon	0.0055	0.0070 (+)	0.0162 (+)	0.0113 (+)	0.0110 (+)
5-RPolygon	0.0062	0.0074 (+)	0.0400 (+)	0.0113 (+)	0.0110 (+)
8-Polygon	0.0046	0.0089 (+)	0.0136 (+)	0.0143 (+)	0.0140 (+)
8-RPolygon	0.0051	0.0093 (+)	0.0747 (+)	0.0144 (+)	0.0138 (+)
10-Polygon	0.0044	0.0072 (+)	0.0123 (+)	0.0120 (+)	0.0112 (+)
10-RPolygon	0.0053	0.0076 (+)	0.0404 (+)	0.0118 (+)	0.0112 (+)
LORD-II vs. others (+/ − / ~)		7/1/0	8/0/0	8/0/0	8/0/0

Table 12: Mean IGDF over 31 independent runs for comparing LORD-II on M -objective polygon and rotated polygon (RPolygon) problems.

M -Problems	LORD-II	NIMMO	TriMOEA _TA&R	MO_Ring_ PSO_SCD	Omni- Optimizer
3-Polygon	0.0023	0.0025 (+)	0.0040 (+)	0.0034 (+)	0.0028 (+)
3-RPolygon	0.0023	0.0025 (+)	0.0046 (+)	0.0034 (+)	0.0028 (+)
5-Polygon	0.0031	0.0044 (+)	0.0149 (+)	0.0057 (+)	0.0051 (+)
5-RPolygon	0.0030	0.0044 (+)	0.0149 (+)	0.0058 (+)	0.0052 (+)
8-Polygon	0.0031	0.0069 (+)	0.0180 (+)	0.0092 (+)	0.0082 (+)
8-RPolygon	0.0032	0.0069 (+)	0.0190 (+)	0.0093 (+)	0.0083 (+)
10-Polygon	0.0033	0.0064 (+)	0.0204 (+)	0.0087 (+)	0.0074 (+)
10-RPolygon	0.0034	0.0064 (+)	0.0185 (+)	0.0086 (+)	0.0075 (+)
LORD-II vs. others (+/ − / ~)		8/0/0	8/0/0	8/0/0	8/0/0

Table 13: Cartesian coordinate plots of the 2-dimensional PSs of M -objective polygon and rotated polygon problems.



approach of LORD, LORD-II is designed for higher number of objectives using PBI function. However, the performance of LORD-II on problems with small number of objectives has not been tested so far. Thus, this experiment compares the performance of LORD, LORD-II and CEC 2019 competition winner [55] (MMO-Clustering PSO⁴).

⁴As mentioned in <http://www5.zzu.edu.cn/ecilab/info/1036/1211.htm> with implementa-

Table 14: Mean \pm Standard Deviation (Rank) of rPSP and rHV for 2-objective MMMOPs over 51 Runs.

Problems	rPSP=IGDX/cov_rate			rHV=1/HV		
	LORD	LORD-II	MMO-Clustering PSO	LORD	LORD-II	MMO-Clustering PSO
MMF1	0.0441 \pm 0.0044	0.0562 \pm 0.0024 (+)	0.0332 \pm 0.0016 (−)	1.0737 \pm 0.0008	1.1480 \pm 0.0004 (+)	1.1456 \pm 0.0003 (+)
MMF1 _z	0.0356 \pm 0.0069	0.0653 \pm 0.0066 (+)	0.0237 \pm 0.0009 (−)	1.0731 \pm 0.0008	1.1466 \pm 0.0005 (+)	1.1454 \pm 0.0002 (+)
MMF1 _e	0.8894 \pm 0.1466	1.6368 \pm 0.5607 (+)	0.5479 \pm 0.0859 (−)	1.0751 \pm 0.0021	1.1532 \pm 0.0018 (+)	1.2560 \pm 0.0376 (+)
MMF2	0.0219 \pm 0.0108	0.0284 \pm 0.0041 (+)	0.1294 \pm 0.0314 (+)	1.0817 \pm 0.0120	1.2168 \pm 0.0067 (+)	1.2605 \pm 0.0177 (+)
MMF3	0.0200 \pm 0.0105	0.0346 \pm 0.0108 (+)	0.0465 \pm 0.0047 (+)	1.0792 \pm 0.0322	1.2527 \pm 0.0689 (+)	1.1920 \pm 0.0042 (+)
MMF4	0.0253 \pm 0.0036	0.0362 \pm 0.0131 (+)	0.0128 \pm 0.0002 (−)	1.5234 \pm 0.0003	1.8545 \pm 0.0005 (+)	1.8510 \pm 0.0010 (+)
MMF5	0.0814 \pm 0.0080	0.0922 \pm 0.0043 (+)	0.0556 \pm 0.0017 (−)	1.0734 \pm 0.0006	1.1481 \pm 0.0002 (+)	1.1456 \pm 0.0004 (+)
MMF6	0.0692 \pm 0.0104	0.0923 \pm 0.0084 (+)	0.0431 \pm 0.0016 (−)	1.0732 \pm 0.0003	1.1472 \pm 0.0012 (+)	1.1453 \pm 0.0004 (+)
MMF7	0.0219 \pm 0.0044	0.0303 \pm 0.0020 (+)	0.0142 \pm 0.0004 (−)	1.0731 \pm 0.0002	1.1458 \pm 0.0005 (+)	1.1445 \pm 0.0004 (+)
MMF8	0.0745 \pm 0.0452	0.0917 \pm 0.0392 (+)	0.0654 \pm 0.0061 (−)	1.7915 \pm 0.0012	2.3794 \pm 0.6116 (+)	2.4027 \pm 0.0060 (+)
MMF9	0.0047 \pm 0.0002	0.0097 \pm 0.0464 (+)	0.0056 \pm 0.0002 (+)	0.0820 \pm 0.0000	0.1172 \pm 0.0005 (+)	0.1032 \pm 0.0000 (+)
MMF10	0.0018 \pm 0.0007	0.0043 \pm 0.0003 (+)	0.0233 \pm 0.0029 (+)	0.0678 \pm 0.0000	0.0811 \pm 0.0002 (+)	0.0797 \pm 0.0001 (+)
MMF11	0.0029 \pm 0.0002	0.0045 \pm 0.0001 (+)	0.0046 \pm 0.0001 (+)	0.0581 \pm 0.0000	0.0738 \pm 0.0002 (+)	0.0690 \pm 0.0000 (+)
MMF12	0.0013 \pm 0.0001	0.0053 \pm 0.0003 (+)	0.0055 \pm 0.0005 (+)	0.5431 \pm 0.0000	0.8312 \pm 0.0041 (+)	0.6686 \pm 0.0115 (+)
MMF13	0.0243 \pm 0.0039	0.2723 \pm 0.0631 (+)	0.0325 \pm 0.0010 (+)	0.0444 \pm 0.0000	0.0550 \pm 0.0002 (+)	0.0544 \pm 0.0000 (+)
Omni-test	0.0754 \pm 0.0242	0.1215 \pm 0.0424 (+)	0.5470 \pm 0.0476 (+)	0.0518 \pm 0.0000	0.0190 \pm 0.0000 (−)	0.0190 \pm 0.0000 (−)
SYM-PART simple	0.0556 \pm 0.0145	0.1191 \pm 0.0206 (+)	0.2801 \pm 0.0370 (+)	0.0520 \pm 0.0000	0.0601 \pm 0.0000 (+)	0.0610 \pm 0.0001 (+)
SYM-PART rotated	0.1730 \pm 0.0743	0.2252 \pm 0.0389 (+)	0.2729 \pm 0.0262 (+)	0.0520 \pm 0.0000	0.0602 \pm 0.0000 (+)	0.0609 \pm 0.0001 (+)
LORD vs. others (+/−/∼)		18/0/0	10/8/0	(+/-/~)	17/1/0	17/1/0

It also uses $n_{pop} = 100N$ and $MaxFES = 5000N$ and considers the rPSP and rHV values for comparison. The performance of all the three MMMOEAs for 2-objective MMMOPs are specified in Table 14 and validated using Wilcoxon’s rank-sum test [48].

According to Table 14, LORD demonstrates superior performance in 17 out of 18 cases in the objective space. In the decision space, LORD outperforms LORD-II in all the 18 cases and the CEC 2019 winner in 10 out of 18 cases. Thus, LORD can be considered as a very robust algorithm for 2-objective MMMOPs.

5) **Experiment-V: Comparison by Variation in Population Size:** While a large population size (n_{pop}) is a necessity for MMMOPs (as mentioned in Section 1), standard MOEAs such as MOEA/DD may have poor performance due to a large n_{pop} . For a fair assessment on the superiority of LORD-II, this experiment compares LORD-II with MOEA/DD using both small n_{pop} (as per the optimal setting of MOEA/DD in [15]) and large n_{pop} ($= 100 \times N$ as per the recommendation of CEC 2019 MMMOPs [4]) in Table 15, from which the following insights are obtained:

- LORD-II is superior even for small n_{pop} .
- While MOEA/DD never outperforms LORD-II in the decision space, the former is marginally superior for a few cases (one out of 16 cases for small n_{pop} and two out of 16 cases for large n_{pop}) in the objective space.

tion obtained from Dr. Weiwei Zhang (anqikeli@163.com).

- A large n_{pop} improves IGDX and IGDF regardless of the effectiveness of the underlying algorithm [29]. This behavior is also observed in Table 15 for both LORD-II and MOEA/DD. However, since the superiority of LORD-II against MOEA/DD is also established for a small n_{pop} , these results indeed reflect the efficient synergism of various strategies in the evolutionary framework of LORD-II.

Table 15: Mean of IGDX and IGDF over 51 independent runs with different population sizes (n_{pop}) for M -objective MMMOPs.

Problems	M	Recommended Population Size for MOEA/DD in [15]						Recommended Population Size for MMMOPs in [4]			
		n_{pop}	IGDX		IGDF		n_{pop}	IGDX		IGDF	
			LORD-II	MOEA/DD	LORD-II	MOEA/DD		LORD-II	MOEA/DD	LORD-II	MOEA/DD
MMF14	3	91	0.0832	0.2150 (+)	0.1044	0.1045 (~)	300	0.0443	0.0671 (+)	0.0540	0.0555 (+)
MMF14 _a	3	91	0.1150	0.2076 (+)	0.1044	0.1045 (~)	300	0.0576	0.0780 (+)	0.0561	0.0568 (+)
MMF15	3	91	0.0514	0.0522 (~)	0.1055	0.1056 (~)	300	0.0287	0.0295 (+)	0.0548	0.0562 (+)
MMF15 _a	3	91	0.0638	0.0705 (+)	0.1056	0.1144 (+)	300	0.0355	0.0357 (~)	0.0571	0.0607 (+)
MMF14	5	210	0.3070	0.3314 (+)	0.3125	0.3136 (+)	495	0.2448	0.2554 (+)	0.0564	0.0598 (+)
MMF14 _a	5	210	0.3283	0.4083 (+)	0.3129	0.3135 (~)	495	0.2670	0.2846 (+)	0.0752	0.0839 (+)
MMF15	5	210	0.2460	0.2652 (+)	0.3155	0.3167 (+)	495	0.1960	0.2032 (+)	0.0602	0.0645 (+)
MMF15 _a	5	210	0.2695	0.2963 (+)	0.3181	0.3168 (-)	495	0.2155	0.2230 (+)	0.0895	0.0999 (+)
MMF14	8	156	0.6864	0.7006 (+)	0.7233	0.7244 (+)	828	0.5621	0.5857 (+)	0.1445	0.1494 (+)
MMF14 _a	8	156	0.6851	0.7363 (+)	0.7225	0.7241 (+)	828	0.5725	0.5936 (+)	0.1776	0.1905 (+)
MMF15	8	156	0.6086	0.6263 (+)	0.7270	0.7291 (+)	828	0.5146	0.5586 (+)	0.1503	0.1486 (-)
MMF15 _a	8	156	0.6543	0.6539 (~)	0.7277	0.7289 (+)	828	0.5315	0.5498 (+)	0.2195	0.2159 (~)
MMF14	10	275	0.8404	0.8847 (+)	0.6811	0.6864 (+)	935	0.7088	0.7373 (+)	0.3463	0.3102 (~)
MMF14 _a	10	275	0.8374	0.8972 (+)	0.6839	0.6907 (+)	935	0.6869	0.7241 (+)	0.4296	0.4317 (~)
MMF15	10	275	0.7787	0.8105 (+)	0.6864	0.6903 (+)	935	0.6469	0.6731 (+)	0.3561	0.2984 (-)
MMF15 _a	10	275	0.8074	0.8246 (+)	0.6913	0.6940 (+)	935	0.6712	0.6848 (+)	0.4375	0.4384 (~)
LORD-II vs. MOEA/DD (+/-/~)			14/0/2		(+/ - / ~)		(+/ - / ~)		15/0/1		(+/ - / ~)

Thus, it is evident that the improved performance is an attribute of the algorithmic framework of LORD-II and not of the large n_{pop} .

4.6 Scalability Study on LORD-II framework

As most of the MMMOEAs are not tested on problems scalable in candidate dimension (N) [27], the scalability of LORD-II is established by studying its performance in Table 16 with variations in N using a 3-objective MMF14 problem for $N = \{3, 10, 30, 50, 100\}$.

From Table 16, the following observations are noted:

- As the number of objectives (M) does not change, the performance of LORD-II remains unaffected in the objective space as noted from the absence of any significant increase in rHV and IGDF.
- For small N , the performance in the decision space deteriorates only linearly (not exponentially) with an increase in N . For example, IGDX increases 34 times when N is increased from 3 to 30. However, with further increase in N ,

Table 16: Mean of rPSP, IGDX, rHV and IGDF for 3-objective MMF14 (with different candidate dimensions, N) over 51 Independent Runs of LORD-II.

N	rPSP	IGDX	rHV	IGDF
3	0.0449	0.0443	1.0395	0.0540
10	0.5928	0.5838	1.0414	0.0013
30	2.8270	1.5038	1.0402	0.0001
50	2.1513	2.1258	1.0405	0.0001
100	3.2476	3.1807	1.0406	0.0000

the deterioration in performance is even less drastic. For example, IGDX only doubles when N is increased from 30 to 100.

Thus, LORD-II, using decomposition of decision and objective spaces, works efficiently even for high-dimensional MMMOPs, i.e., LORD-II is scalable with problem size.

5 Conclusion and Future Research Directions

As most of the existing MMMOEAs evaluates crowding distance over the entire decision space, its analysis exhibits a major disadvantage which is identified as the crowding illusion problem (Section 2.1). To mitigate the adverse effects of this problem for MMMOPs, a novel evolutionary framework is presented in this manuscript. It is a first of its kind algorithm to attempt decomposition of decision space using graph Laplacian based clustering for maintaining the diversity of solutions in that space. It uses reference vectors to partition the objective space for maintaining diversity in the objective space. The proposed algorithm has two different versions which differently impart the selection pressure on the population. The first version (LORD) is for MMMOPs with small number of objectives, which eliminates the maximally crowded solution from the last non-dominated rank. The second version (LORD-II) is for problems with higher number of objectives which eliminates the candidate with maximal PBI, from the maximally large cluster. During elimination of candidate, LORD and LORD-II try to ensure that the removal does not occur from the sub-spaces (defined by reference vectors) with only one associated candidate. The proposed frameworks have been tested over several MMMOPs [4] and MMMaOPs [4, 30] and their performance have been compared with recent state-of-the-art algorithms to establish their efficacy.

Inspite of their superior performance, LORD and LORD-II have the following disadvantages; reducing the effects of which could be considered for future extensions of this work:

1. Spectral clustering solves the preliminary purpose of decomposing the decision space and is effective for problems like MMF2, MMF3, SYM-PART, etc. However, for problems like MMF1, MMF6, MMF7, etc., where overlap exists along certain dimensions within each subset of PS [4], spectral clustering does not completely eliminate the crowding illusion problem (Section 2.1). Hence, the search for better decomposition methods (with adaptive threshold/parameters) in the decision space forms a potential future work.
2. As done in the proposed work as well as in most of the previous works such as [25, 8], the mating pool selection is performed from neighboring candidates in the objective space. Nonetheless, if an approximate partitioning of the decision space could be done to yield the bounding box of each subset of PS, intra- and inter-subset mating could further be studied for enhanced diversity of solutions in the decision space. Moreover, different subsets of the PS of an MMMOP have correlated structures. Such information on correlation could be incorporated to design new perturbation operators for guiding the search in MMMOPs.
3. It should be noted that the research on MMMOPs has just started developing. Hence, besides designing more algorithms to deal with MMMOPs, other challenges in this new direction involve developing novel decision-making strategies (selecting one out of multiple equivalent solutions from the PS mapping to a certain solution in the PF), analyzing more practical problems, designing more difficult benchmark problems (e.g., CEC 2020 test suite [56]), validating existing approaches on such problems as well as designing new performance measures (independent of the true PS) to study the convergence and diversity in the decision space for practical problems.

References

- [1] Aimin Zhou, Bo-Yang Qu, Hui Li, Shi-Zheng Zhao, Ponnuthurai Nagarathnam Suganthan, and Qingfu Zhang. Multiobjective evolutionary algorithms: A survey of the state of the art. *Swarm and Evolutionary Computation*, 1(1):32–49, 2011.
- [2] Anirban Mukhopadhyay, Ujjwal Maulik, Sanghamitra Bandyopadhyay, and Carlos Artemio Coello Coello. A survey of multiobjective evolutionary algorithms for data mining: Part I. *IEEE Transactions on Evolutionary Computation*, 18(1):4–19, Feb 2014.
- [3] Ryoji Tanabe and Hisao Ishibuchi. A review of evolutionary multi-modal multi-objective optimization. *IEEE Transactions on Evolutionary Computation*, pages 1–9, 2019.

- [4] J. J. Liang, B. Y. Qu, D. W. Gong, and C. T. Yue. Problem definitions and evaluation criteria for the CEC 2019 special session on multimodal multiobjective optimization. *Technical Report, Computational Intelligence Laboratory, Zhengzhou University*, 2019.
- [5] Fumiya Kudo, Tomohiro Yoshikawa, and Takeshi Furuhashi. A study on analysis of design variables in pareto solutions for conceptual design optimization problem of hybrid rocket engine. In *2011 IEEE Congress of Evolutionary Computation (CEC)*, pages 2558–2562, June 2011.
- [6] C. T. Yue, J. J. Liang, B. Y. Qu, K. J. Yu, and H. Song. Multimodal multiobjective optimization in feature selection. In *2019 IEEE Congress on Evolutionary Computation (CEC)*, pages 302–309, June 2019.
- [7] Jafar Jamal, Roberto Montemanni, David Huber, Marco Derboni, and Andrea E Rizzoli. A multi-modal and multi-objective journey planner for integrating carpooling and public transport. *Journal of Traffic and Logistics Engineering*, 5(2):68–72, December 2017.
- [8] Monalisa Pal and Sanghamitra Bandyopadhyay. Differential evolution for multimodal multi-objective problems. In *Proceedings of the Genetic and Evolutionary Computation Conference Companion, GECCO '19*, pages 1399–1406, New York, NY, USA, 2019. ACM.
- [9] K. Deb, A. Pratap, S. Agarwal, and T. Meyarivan. A fast and elitist multiobjective genetic algorithm: NSGA-II. *IEEE Transactions on Evolutionary Computation*, 6(2):182–197, 2002.
- [10] Y. Yuan, X. Hua, W. Bo, and Y. Xin. A new dominance relation-based evolutionary algorithm for many-objective optimization. *IEEE Transactions on Evolutionary Computation*, 20(1):16–37, 2016.
- [11] Johannes Bader and Eckart Zitzler. HypE: An algorithm for fast hypervolume-based many-objective optimization. *Evolutionary computation*, 19(1):45–76, 2011.
- [12] Adriana Menchaca-Mendez and Carlos A Coello Coello. GDE-MOEA: a new moea based on the generational distance indicator and ε -dominance. In *2015 IEEE Congress on Evolutionary Computation (CEC)*, pages 947–955. IEEE, 2015.

- [13] Z. Qingfu and L. Hui. MOEA/D: A multiobjective evolutionary algorithm based on decomposition. *IEEE Transactions on Evolutionary Computation*, 11(6):712–731, 2007.
- [14] Kalyanmoy Deb and Himanshu Jain. An evolutionary many-objective optimization algorithm using reference-point-based nondominated sorting approach, part I: Solving problems with box constraints. *IEEE Transactions on Evolutionary Computation*, 18(4):577–601, 2014.
- [15] Ke Li, Kalyanmoy Deb, Qingfu Zhang, and Sam Kwong. An evolutionary many-objective optimization algorithm based on dominance and decomposition. *IEEE Transactions on Evolutionary Computation*, 19(5):694–716, 2015.
- [16] I. Das and J. E. Dennis. Normal-boundary intersection: A new method for generating the pareto surface in nonlinear multicriteria optimization problems. *SIAM Journal on Optimization*, 8(3):631–657, 1998.
- [17] Qi Kang, Xinyao Song, MengChu Zhou, and Li Li. A collaborative resource allocation strategy for decomposition-based multiobjective evolutionary algorithms. *IEEE Transactions on Systems, Man, and Cybernetics: Systems*, 49(12):2416–2423, Dec 2019.
- [18] Kalyanmoy Deb and Santosh Tiwari. Omni-optimizer: A procedure for single and multi-objective optimization. In Carlos A. Coello Coello, Arturo Hernández Aguirre, and Eckart Zitzler, editors, *Evolutionary Multi-Criterion Optimization*, pages 47–61, Berlin, Heidelberg, 2005. Springer Berlin Heidelberg.
- [19] K. P. Chan and T. Ray. An evolutionary algorithm to maintain diversity in the parametric and the objective space. In *International Conference on Computational Robotics and Autonomous Systems (CIRAS), Centre for Intelligent Control, National University of Singapore*, 2005.
- [20] Aimin Zhou, Qingfu Zhang, and Yaochu Jin. Approximating the set of pareto-optimal solutions in both the decision and objective spaces by an estimation of distribution algorithm. *IEEE Transactions on Evolutionary Computation*, 13(5):1167–1189, 2009.
- [21] J. J. Liang, C. T. Yue, and B. Y. Qu. Multimodal multi-objective optimization: A preliminary study. In *2016 IEEE Congress on Evolutionary Computation (CEC)*, pages 2454–2461. IEEE, 2016.
- [22] Mahrokh Javadi, Heiner Zille, and Sanaz Mostaghim. Modified crowding distance and mutation for multimodal multi-objective optimization. In *Proceedings of the*

- Genetic and Evolutionary Computation Conference Companion*, GECCO '19, pages 211–212, New York, NY, USA, 2019. ACM.
- [23] Caitong Yue, Boyang Qu, and Jing Liang. A multiobjective particle swarm optimizer using ring topology for solving multimodal multiobjective problems. *IEEE Transactions on Evolutionary Computation*, 22(5):805–817, Oct 2018.
 - [24] Qinqin Fan and Xuefeng Yan. Solving multimodal multiobjective problems through zoning search. *IEEE Transactions on Systems, Man, and Cybernetics: Systems*, pages 1–12, 2019.
 - [25] Ryoji Tanabe and Hisao Ishibuchi. A decomposition-based evolutionary algorithm for multi-modal multi-objective optimization. In Anne Auger, Carlos M. Fonseca, Nuno Lourenço, Penousal Machado, Luís Paquete, and Darrell Whitley, editors, *Parallel Problem Solving from Nature – PPSN XV*, pages 249–261, Cham, 2018. Springer International Publishing.
 - [26] Ryoji Tanabe and Hisao Ishibuchi. A framework to handle multimodal multi-objective optimization in decomposition-based evolutionary algorithms. *IEEE Transactions on Evolutionary Computation*, 24(4):720–734, 2020.
 - [27] Yiping Liu, Gary G. Yen, and Dunwei Gong. A multi-modal multi-objective evolutionary algorithm using two-archive and recombination strategies. *IEEE Transactions on Evolutionary Computation*, 23(4):660–674, Aug 2019.
 - [28] K. Maity, R. Sengupta, and S. Saha. MM-NAEMO : Multimodal neighborhood-sensitive archived evolutionary many-objective optimization algorithm. In *2019 IEEE Congress on Evolutionary Computation (CEC)*, pages 286–294, June 2019.
 - [29] Ryoji Tanabe and Hisao Ishibuchi. A niching indicator-based multi-modal many-objective optimizer. *Swarm and Evolutionary Computation*, 49:134 – 146, 2019.
 - [30] Hisao Ishibuchi, Naoya Akedo, and Yusuke Nojima. A many-objective test problem for visually examining diversity maintenance behavior in a decision space. In *Proceedings of the 13th Annual Conference on Genetic and Evolutionary Computation*, GECCO '11, pages 649–656, New York, NY, USA, 2011. ACM.
 - [31] Raunak Sengupta, Monalisa Pal, Sriparna Saha, and Sanghamitra Bandyopadhyay. NAEMO: Neighborhood-sensitive archived evolutionary many-objective optimization algorithm. *Swarm and Evolutionary Computation*, 46:201 – 218, 2019.

- [32] Li-Min Li, Kang-Di Lu, Guo-Qiang Zeng, Lie Wu, and Min-Rong Chen. A novel real-coded population-based extremal optimization algorithm with polynomial mutation: A non-parametric statistical study on continuous optimization problems. *Neurocomputing*, 174:577 – 587, 2016.
- [33] Xianpeng Wang, Zhiming Dong, and Lixin Tang. Multiobjective differential evolution with personal archive and biased self-adaptive mutation selection. *IEEE Transactions on Systems, Man, and Cybernetics: Systems*, pages 1–13, 2018.
- [34] Raunak Sengupta and Sriparna Saha. Reference point based archived many objective simulated annealing. *Information Sciences*, 467:725 – 749, 2018.
- [35] Tea Robič and Bogdan Filipič. DEMO: Differential evolution for multiobjective optimization. In C. A. C. Coello, A. H. Aguirre, and E. Zitzler, editors, *Evolutionary Multi-Criterion Optimization*, pages 520–533, Berlin, Heidelberg, 2005. Springer Berlin Heidelberg.
- [36] A. K. Qin and P. N. Suganthan. Self-adaptive differential evolution algorithm for numerical optimization. In *Evolutionary Computation, 2005. The 2005 IEEE Congress on*, volume 2, pages 1785–1791. IEEE, 2005.
- [37] Ulrike von Luxburg. A tutorial on spectral clustering. *Statistics and Computing*, 17(4):395–416, Dec 2007.
- [38] Aparajita Khan and Pradipta Maji. Approximate graph laplacians for multimodal data clustering. *IEEE Transactions on Pattern Analysis and Machine Intelligence*, pages 1–16, 2019.
- [39] Jeff Cheeger. A lower bound for the smallest eigenvalue of the Laplacian. In Robert C. Gunning, editor, *Problems in analysis (Papers dedicated to Salomon Bochner, 1969)*, pages 195–199. Princeton Univ. Press, Princeton, NJ, 1970.
- [40] Peter Buser. Über eine ungleichung von Cheeger (On an inequality of Cheeger). *Mathematische Zeitschrift (in German)*, 158(3):245–252, Oct 1978.
- [41] Michael B. Cohen, Sam Elder, Cameron Musco, Christopher Musco, and Madalina Persu. Dimensionality reduction for k-means clustering and low rank approximation. In *Proceedings of the Forty-seventh Annual ACM Symposium on Theory of Computing*, STOC ’15, pages 163–172, New York, NY, USA, 2015. ACM.
- [42] Abdelkarim Ben Ayed, Mohamed Ben Halima, and Adel M Alimi. Adaptive fuzzy exponent cluster ensemble system based feature selection and spectral clustering.

- In *2017 IEEE International Conference on Fuzzy Systems (FUZZ-IEEE)*, pages 1–6. IEEE, 2017.
- [43] Sumit Mishra, Mondal. Samrat, and Sriparna Saha. Fast implementation of steady-state NSGA-II. In *2016 IEEE Congress on Evolutionary Computation (CEC)*, pages 3777–3784, July 2016.
 - [44] Monalisa Pal and Sanghamitra Bandyopadhyay. ESOEA: Ensemble of single objective evolutionary algorithms for many-objective optimization. *Swarm and Evolutionary Computation*, 50:100511, 2019.
 - [45] C. A. C. Coello. Recent results and open problems in evolutionary multiobjective optimization. In C. Martín-Vide, R. Neruda, and M. A. Vega-Rodríguez, editors, *Theory and Practice of Natural Computing*, pages 3–21, Cham, 2017. Springer International Publishing.
 - [46] S. Bandyopadhyay and A. Mukherjee. An algorithm for many-objective optimization with reduced objective computations: A study in differential evolution. *IEEE Transactions on Evolutionary Computation*, 19(3):400–413, 2015.
 - [47] Raunak Sengupta, Monalisa Pal, Sriparna Saha, and Sanghamitra Bandyopadhyay. Population dynamics indicators for evolutionary many-objective optimization. In *Progress in Advanced Computing and Intelligent Engineering*, pages 261–271. Springer, 2019.
 - [48] Ye Tian, Ran Cheng, Xingyi Zhang, Fan Cheng, and Yaochu Jin. An indicator based multi-objective evolutionary algorithm with reference point adaptation for better versatility. *IEEE Transactions on Evolutionary Computation*, 2017.
 - [49] Ye Tian, Xingyi Zhang, Ran Cheng, and Yaochu Jin. A multi-objective evolutionary algorithm based on an enhanced inverted generational distance metric. In *2016 IEEE Congress on Evolutionary Computation (CEC)*, pages 5222–5229, July 2016.
 - [50] Anirban Mukhopadhyay, Ujjwal Maulik, Sanghamitra Bandyopadhyay, and Carlos Artemio Coello Coello. Survey of multiobjective evolutionary algorithms for data mining: Part II. *IEEE Transactions on Evolutionary Computation*, 18(1):20–35, Feb 2014.
 - [51] S. Das, S. S. Mullick, and P. N. Suganthan. Recent advances in differential evolution – an updated survey. *Swarm and Evolutionary Computation*, 27:1 – 30, 2016.

- [52] K. Deb and R. B. Agrawal. Simulated binary crossover for continuous search space. *Complex systems*, 9(2):115–148, 1995.
- [53] Tea Tušar and Bogdan Filipič. Differential evolution versus genetic algorithms in multiobjective optimization. In Shigeru Obayashi, Kalyanmoy Deb, Carlo Poloni, Tomoyuki Hiroyasu, and Tadahiko Murata, editors, *Evolutionary Multi-Criterion Optimization*, pages 257–271, Berlin, Heidelberg, 2007. Springer Berlin Heidelberg.
- [54] Zhenan He and Gary G Yen. Visualization and performance metric in many-objective optimization. *IEEE Transactions on Evolutionary Computation*, 20(3):386–402, June 2016.
- [55] C.T. Yue, J.J. Liang, P.N. Suganthan, B.Y. Qu, K.J. Yu, and S. Liu. MMOGA for solving multimodal multiobjective optimization problems with local pareto sets. In *2020 IEEE Congress on Evolutionary Computation (CEC)*, pages 1–8. IEEE, 2020.
- [56] J. J. Liang, P. N. Suganthan, B. Y. Qu, D. W. Gong, and C. T. Yue. Problem definitions and evaluation criteria for the CEC 2020 special session on multi-modal multiobjective optimization. *Technical Report 201912, Computational Intelligence Laboratory, Zhengzhou University, Zhengzhou China And Technical Report, Nanyang Technological University, Singapore*, 2019.